Evaluation of an Encapsulation and Epoxy Resin Injection Procedure for Rehabilitating Corroding Reinforced Concrete Structures

by

Muhammed Alp Ünal and James O. Jirsa

Report on a project sponsored by

Hardcore Dupont Composites
and
The Dow Chemical Company

PMFSEL Report 98-3
Ferguson Structural Engineering Laboratory
The University of Texas at Austin

September 1998

PHIL M. FERGUSON STRUCTURAL ENGINEERING LABORATORY
Department of Civil Engineering / Bureau of Engineering Research
The University of Texas at Austin

Evaluation of an Encapsulation and Epoxy Resin Injection Procedure for Rehabilitating Corroding Reinforced Concrete Structures

by

Muhammed Alp Ünal and James O. Jirsa

Report on a project sponsored by

Hardcore Dupont Composites
and
The Dow Chemical Company

PMFSEL Report 98-3
Ferguson Structural Engineering Laboratory
The University of Texas at Austin

September 1998

Executive Summary

Evaluation of an Encapsulation and Epoxy Injection Procedure for Rehabilitating Corrosion-Damaged Reinforced Concrete Structures

A rehabilitation technique was studied that involved encapsulation with a fiber composite shell and injection of epoxy vinyl ester resin was studied. The technique was used on specimens reinforced with both epoxy-coated bars and with uncoated bars that had been exposed to a corrosive environment for four and a half years. Well-documented, advanced corrosion was evident in the beams. The behavior of specimens encapsulated and injected with resin was compared with specimens that were not repaired. All specimens were exposed to corrosive environment for one additional year. The specimens were monitored by taking half-cell potential readings during the exposure period. At the end of the study, all specimens were examined (bars removed) to assess the condition of the reinforcement. No attempt was made to assess the strength of the beam specimens with or without the composite shell.

Based on the experimental results from this project, the following conclusions were made:

- The use of a fiber reinforced composite shell coupled with epoxy vinyl ester resin injection was not effective in arresting active corrosion in beams damaged from exposure to a corrosive environment for four and a half years prior to repair. The performance of concrete elements similarly encapsulated prior to any exposure and with no corrosion damage could not be assessed in this study.
- Evacuation of the concrete specimens did not remove moisture from the beams and vacuum injection of resin did not result in penetration of resin other than at large cracks. It is likely that moisture was trapped inside the concrete during encapsulation. Since sufficient oxygen and chlorides were present in the concrete, corrosion continued at about the same rate as before repair.
- The encapsulation process covered the concrete surface and eliminated the possibility of inspecting the specimens for rust stains or other signs of corrosion.
- Epoxy-coated bars performed well in all specimens. Uncoated bars showed considerable corrosion damage in both control and encapsulated specimens.

Acknowledgements

Hardcore DuPont Composites and Dow Chemical Company provided the funding to conduct the study. The interest and cooperation of Grant Corboy, Mac Puckett, and David Ridley were essential for the completion of the project. The Texas Department of Transportation made the specimens used in a project that was concluding available for this study. The support of these organizations and individuals is gratefully acknowledged.

The research was conducted as part of the program for a Master of Science degree by Mr. Unal and was supervised by Dr. Jirsa.

Table of Contents

List of Figures

List of Tables

CHAPTER 1

INTRODUCTION

1.1 BACKGROUND

Damage due to corrosion of reinforcement in structural concrete results in very large repair and rehabilitation efforts. Construction costs to protect against corrosion and to ameliorate corrosion damage are significant and estimates range into billions of dollars. In addition, corrosion damage leads to reduced safety for occupants and users of exposed facilities.

Corrosion has always been a concern for structures exposed directly or indirectly to seawater. When extensive use of salt on highways and bridges began in 1960s, tracking of chloride-containing deicing chemicals by vehicles onto concrete structures containing calcium chloride or other chloride-based admixtures created similar corrosion problems in many location away from marine environments [Gibson, 1987]. Parking structures are particularly vulnerable to corrosion due to the transportation of chemicals by vehicles. There are many other cases where corrosion in reinforced concrete structures may be produced by other actions; such as chemical exposure, pollution, and sulfate attack [Nene, 1985].

Repair and rehabilitation of corrosion damaged structures is becoming increasingly important because the deterioration rate of existing structures increases with age. Therefore, research is being conducted in order to find new and efficient ways to protect against corrosion and to repair and rehabilitate structures with corrosion damage.

1.2 REPAIR AND REHABILITATION OF CORROSION DAMAGE

1.2.1 Conventional Methods [Pfeifer, 1985b]

Depending on the degree of corrosion damage, there are several different procedures for repairing corrosion damage.

If corrosion-related distress has progressed to serious spalling, repair procedures generally involve most of the following:

- Removing unsound concrete and exposing reinforcing steel,
- Cleaning concrete and steel by using gutblasting,
- Restoring reinforcement by replacing corroded bars if there is significant loss of steel area,
- Protecting reinforcement,
- Using one of several patching techniques to restore concrete, usually to or exceeding the quality of the original concrete, and
- Applying an appropriate surface coating to the concrete.

If no spalling has occurred, pressure injection of epoxy alone may be a suitable repair procedure for structural cracks and corroded areas where only minor damage is evident. If the cracks are active, however, a flexible material such as an elastomeric joint sealant may be required.

1.2.2 Advantages and Disadvantages of Conventional Repair Materials

Selection of materials and installation procedures is one of the most important aspects of corrosion repair. The selection of materials and procedures must take into account that repairs to one part of the structure should not aggravate corrosion in other parts of the structure [Maurisin, 1985]. The advantages and disadvantages of materials for corrosion-damage are tabulated by Pfeifer [1985b] and given in Table 1.1. Even though this table is for corrosion-damaged vertical surfaces, it provides a very good summary of conventional repair materials or processes.

Table 1.1 Repair Materials for Corrosion-Damaged Vertical Surfaces

Description of material or process	Advantages	Disadvantages	Comments
Shotcrete- a mixture of water, cement, and aggregate combined and sprayed or gunned at high velocity onto the surface to be restored.	Only limited forming needed; bond to properly prepared old concrete is usually excellent.	Rebound; a significant amount of material bounces away from the surface being shotcreted and is thereby lost.	Reinforcement of patch with welded wire fabric or small diameter wire mesh advised.
Hand-applied latex- or polymer-modified portland cement mortar. Several commercially prepared products available.	Low permeability to water; good bond to properly prepared old concrete. High durability, crack resistance, and tensile strength.	Relatively high cost. Not extensively tested in vertical repairs.	Forming not required. Applied with trowel or spatula.
Low water-cement ratio concrete with entrained air and appropriate admixtures to produce a dense workable mix.	Lower cost for repair material, of particular importance for large repairs.	Forms are necessary, and may be difficult to support in some installations.	Water reducing admixtures suggested; superplasticizers may be appropriate. Check for compatibility with air entraining admixture.
Polymer concrete and mortars such as methyl methacrylate and epoxy concretes.	High strength, high durability, and good bond to properly prepared concrete.	Relatively expensive; forms needed for deep repairs. Some are flammable and toxic.	Detailed attention to manufacturer's recommendations required. Careful formulation needed to avoid problems due to differences of physical properties from those of adjoining concrete.
Epoxy injection-crack surface sealed except for injection ports inserted at intervals along crack. Epoxy is then pumped through ports. Proprietary pressurized systems available.	Very little surface preparation needed; strong bond and durability of patch.	Scar marks may be left on surface where crack was injected. Limited to areas where concrete had not yet spalled.	Structural quality bond is established but if large structural movements still occurring, new cracks may open.

1.2.3 New Techniques

With increasing knowledge of corrosion mechanisms and developments in new materials, many techniques for repair of corrosion damage are being implemented or evaluated for future use. Fiber reinforced composite plates in combination with injection of resins or epoxies are being utilized.

Encapsulation has proven to be useful for seismic repair and rehabilitation of structures. These techniques have been used for seismic upgrading of bridge piers for strength and ductility in California [Roberts, 1997].

1.3 THE CORROSION PROCESS

1.3.1 Definition [Fontana, 1986; Speller, 1952]

Corrosion is the deterioration or destruction of a metal by direct chemical or electrochemical reaction with its environment.

1.3.2 Corrosion Process of Reinforcing Steel in Concrete

Corrosion of reinforcing steel in concrete is a well understood process that involves steel, oxygen, and an electrode. Especially in the regions of high humidity or on highway bridges subjected to freeze-thaw cycles treated with sodium chloride, the presence of chlorides turns concrete into an electrolyte. Galvanic currents that develop destroy the passivity or the protective film protecting the steel bar embedded in concrete and convert a small portion of the bar into an anode and a larger part of it into a cathode [Fontana, 1986; Gallegos, 1987].

The single bar corrosion process (Figure 1.1) involves metal dissolution at the anode and oxygen reduction or hydrogen gas evolution along the cathode depending upon the corrosive environment [5]. These reactions are given by Equations 1.1 through 1.3. The corrosion of reinforcing steel is an electrochemical process in which an accompanying flow of electricity is generated. Corrosion leads to the formation of extremely unstable ferric oxide (Equation 1.4), which in the presence of oxygen, produces a corrosion product (rust) through a secondary chemical process (Equation 1.5) that occupies a much greater volume than the reinforcing steel. As a result, strong internal forces are developed and may cause concrete cracks to form parallel to the bar. Carbon dioxide is available at the crack and carbonation penetrates deeper into the concrete to speed up the process. Loss of reinforcing steel area through corrosion will weaken the system and produce structural disintegration and failures [Gallegos, 1987] over the long term.

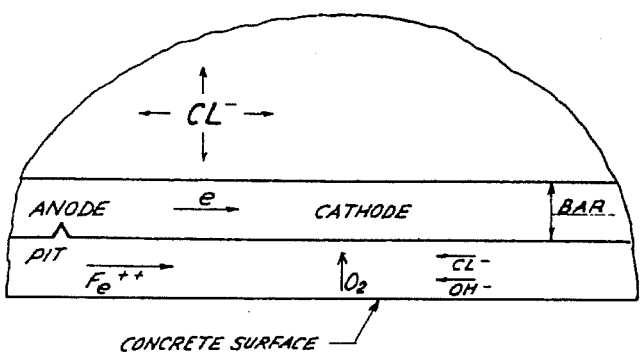

Figure 1.1 Single Bar Corrosion Process [Gallegos, 1987].

Anodic Reaction:

$Fe - 2e^- \rightarrow Fe^{+2}$ Metal Dissolution (Equation 1.1)

Cathodic Reaction:

$2H_2O + O_2 + 4e^- \rightarrow 4OH^-$ Reduction of Oxygen (Equation 1.2)

or $2H^+ + 2e^- \rightarrow H_2$ Hydrogen Gas Evolution (Equation 1.3)

$2Fe + 2H_2O + O_2 \rightarrow 2Fe(OH)_2$ Formation of ferrous oxide (Equation 1.4)

$2Fe(OH)_2 \xrightarrow{O_2, H_2O} 2Fe(OH)_3$ Formation of rust (Equation 1.5)

1.3.3 Factors Contributing to Corrosion Damage

Pfeifer [1985a] discusses the factors contributing to corrosion damage as:

- Age of the structure,
- Orientation of the concrete, i.e., the severity of environment on different faces of the structure due to wind, rain, etc.,
- Corrosive environment,
- Insufficient concrete cover on steel,
- Presence of dissimilar electrically conductive metals, i.e., galvanic coupling,
- Significant amounts of soluble chloride ions in the concrete,
- Permeability of concrete cover,
- Condition of previous repairs to concrete.

1.4 Objective of This Study

The main objective of this study is to evaluate encapsulation and epoxy injection of corrosion damaged reinforced concrete structures to extend their service life. The encapsulation and epoxy injection procedure evaluated in this study was developed by Hardcore DuPont Composites.

The encapsulation and epoxy injection methods are used widely in seismic zones for upgrading strength and ductility but the durability aspects of the procedure have not been studied in depth. The findings of this study are expected to aid in the repair of corrosion damaged reinforced concrete structures and to provide guidelines for using encapsulation and epoxy injection techniques for corrosion protection.

1.5 Scope

Six beams and five macro-cells were included in the test program. The specimens had been exposed to a corrosive environment for four and a half years. Well-documented corrosion data were available and were used in this project. The results from specimens repaired using the encapsulation and epoxy injection were compared with the results from companion unrepaired (control) specimens. All specimens were exposed to a corrosive environment of 3.5 percent by weight saline solution for one year. The same saline solution was used for the previous four and a half year exposure. Specimens were exposed to the saline solution as follows: 3 weeks dry, 1 week wet for the beams, and 2 weeks dry, 2 weeks wet for the macro-cells. The exposure cycle was intended to accelerate corrosion activity.

CHAPTER 2

EXPOSURE HISTORY OF BEAMS AND MACRO-CELLS

2.1 GENERAL

Beams and macro-cells used in the program were cast in 1993 by Kahhaleh [1994] as a part of a study to evaluate the corrosion performance of epoxy-coated reinforcement. A total of 34 beams and 68 macro-cells were included in that study, and six beams and five macro-cells were retained for use in this program.

2.2 BEAMS

2.2.1 Properties

The reinforced concrete beams were designed to simulate cracked, loaded concrete components exposed to high corrosive environments for assessing the durability of epoxy-coated bars. The beams are 200 mm. (8 in.) by 300 mm. (12 in.) in cross section and 2.9 m. (9 ft.) long. There are two 10 mm. (#3) black (uncoated) bars at the top and two 19 mm. (#6) epoxy-coated bars at the bottom. Also there is a 10-mm. epoxy-coated stirrup in the middle of the beams to support the beam longitudinal reinforcement. A detail of the cross section is shown in Figure 2.1.

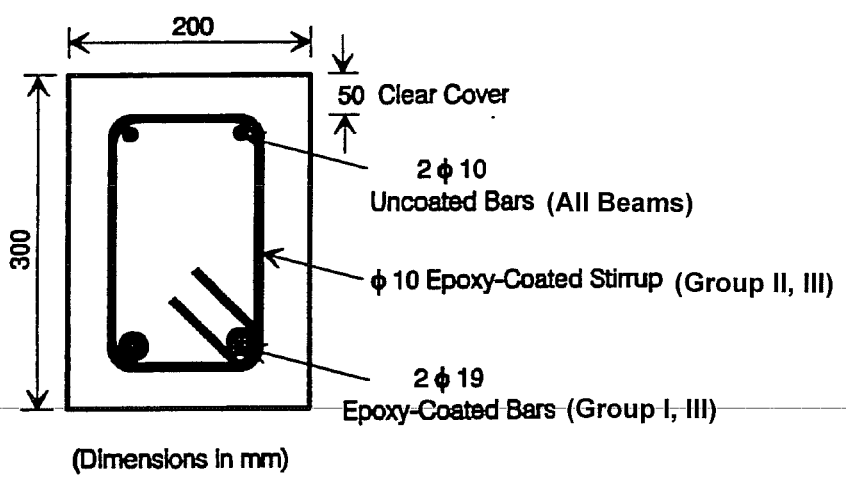

Figure 2.1 Cross Section of the Beams and Bars Exposed [Kahhaleh, 1994].

In the previous test program, 3 groups of beams (I, II, and III) were studied. Details of group I, II, and III beams are shown in Figure 2.2, Figure 2.3, and Figure 2.4 respectively. A high permeability concrete was used in order to allow chlorides to penetrate into the concrete easily. The compressive strength-time curves for each group are shown in Figure 2.5. In addition to differences between groups, there are differences for beams within a group. In some beams the epoxy-coated reinforcement was damaged intentionally and left in a damaged condition while it was patched in

other beams. In a few beams the coated bars were used as received. The cracking condition varied by not loading some beams (uncracked), loading and then removing the load (closed cracks), and loaded with the load maintained during the exposure cycle (open cracks). Table 2.1 summarizes the properties for all 6 beams used in the encapsulation and epoxy injection study. A description of the prior cracking condition (loading history) and for this study is also provided.

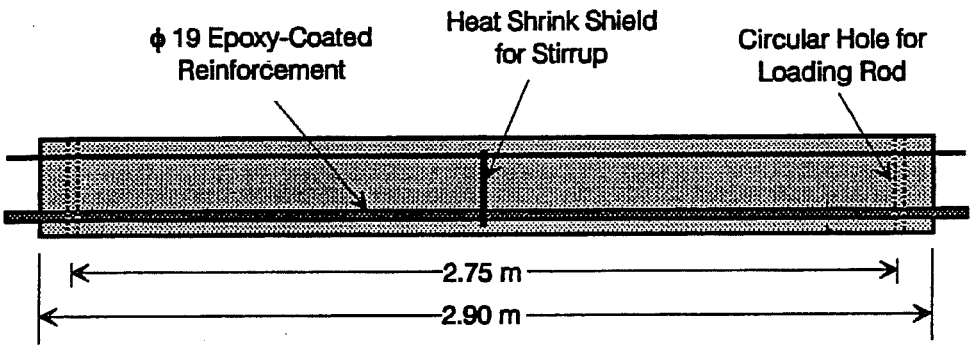

Figure 2.2 Details of Group I-Beam Specimen (Longitudinal Steel) [Kahhaleh, 1994].

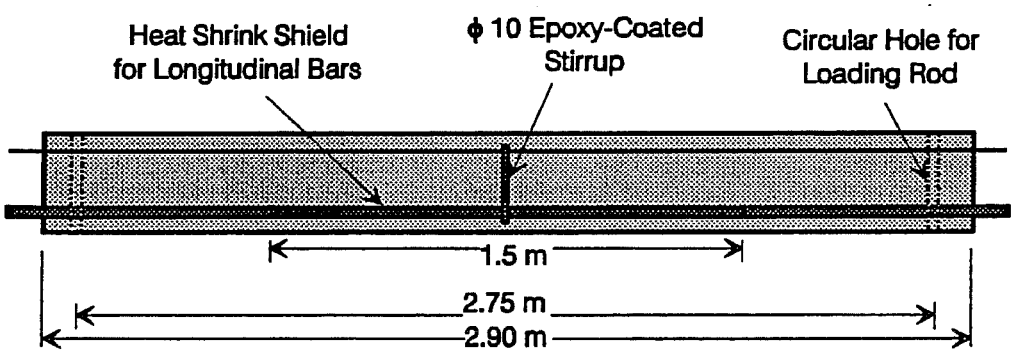

Figure 2.3 Details of Group II Beam Specimen (Stirrup) [Kahhaleh, 1994].

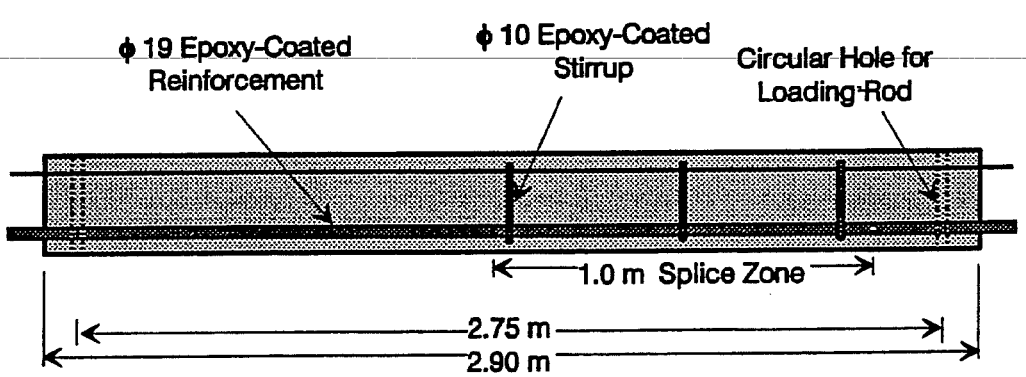

Figure 2.4 Details of Group III Beam Specimen (All Bars) [Kahhaleh, 1994].

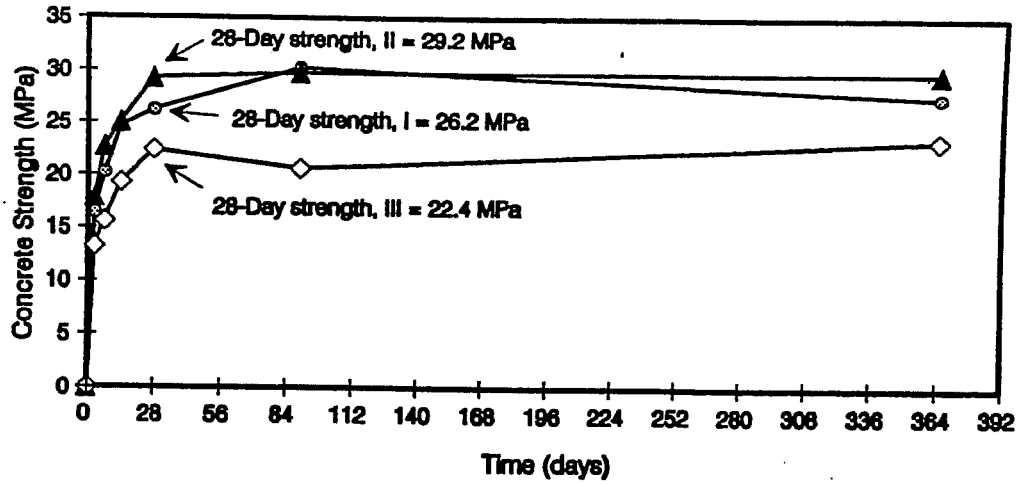

Figure 2.5 Concrete Strength-Time Curve for Beam Groups. [Kahhaleh, 1994]

Table 2.1 Summary of Beam Conditions.

BEAM	GROUP/ PROPERTIES	COATING CONDITION, DAMAGE LEVEL	CRACKING CONDITION		TYPE
			Previous Study	This Study	
B3	Group I Monitoring Longitudinal Bars (Stirrups were Covered)	As Received	Closed	Closed	Encapsulated
B6	Group I Monitoring Longitudinal Bars (Stirrups were Covered)	As Received	Open	Open	Encapsulated
B12	Group I Monitoring Longitudinal Bars (Stirrups were Covered)	3% Damaged	Open	Open	Control
B19	Group II Monitoring Stirrups (Longitudinal Bars were Covered)	As Received	Open	Closed	Encapsulated
B30	Group III Monitoring Longitudinal Bars and One Stirrup	Both Longitudinal Bars and Stirrups had 3% Damaged and Were Patched	Closed	Open	Control
B34	Group III Monitoring Longitudinal Spliced Bars and Three Stirrups	Stirrup 3% Damaged, Stirrup and Splice Bar End Was Patched	Open	Open	Encapsulated

2.2.2 Test Setup

Pairs of beams were loaded back to back as shown in Figure 2.6. Figures 2.7 and 2.8 show the beams under test and during loading.

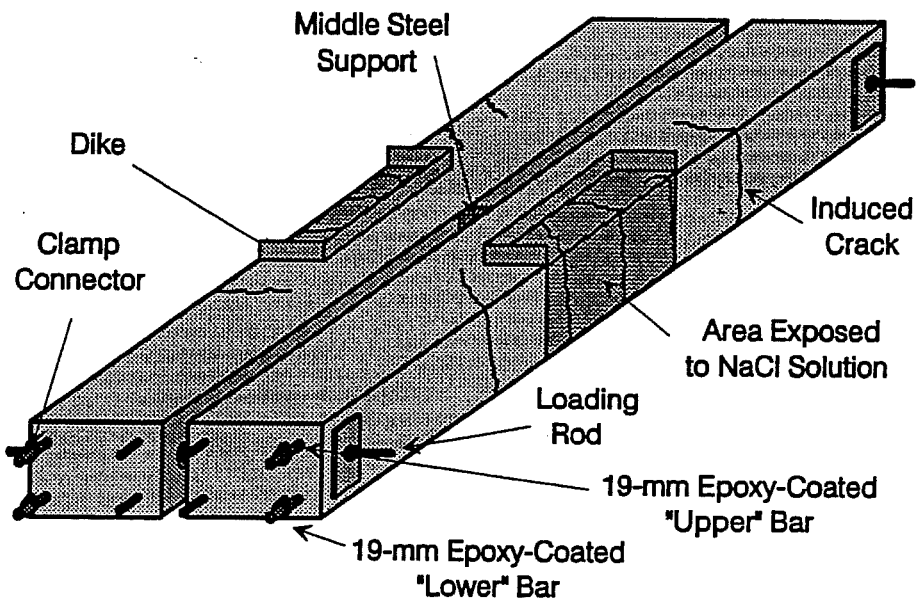

Figure 2.6 Model of Beam Exposure Test Specimens [Kahhaleh, 1994].

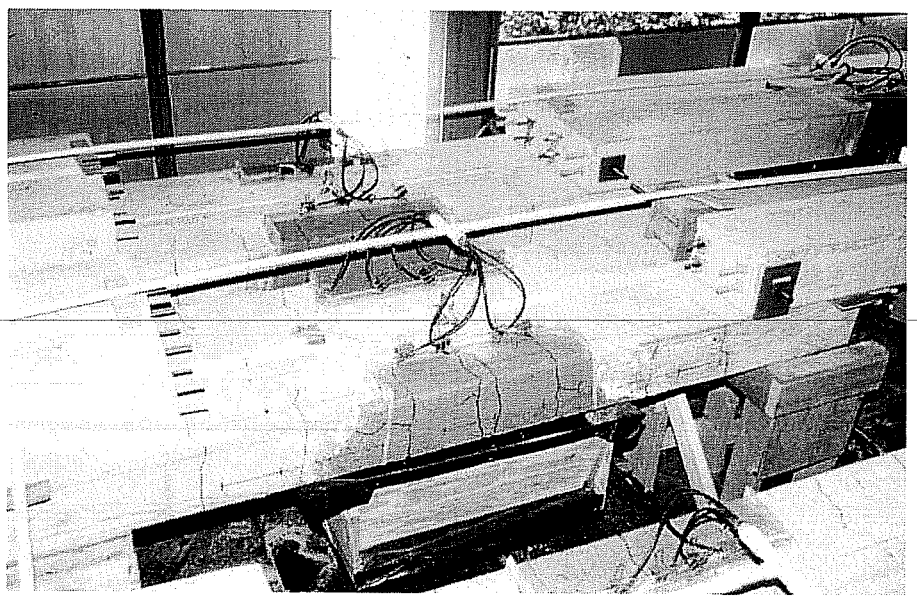

Figure 2.7 Beam Exposure Test Setup [Kahhaleh, 1994].

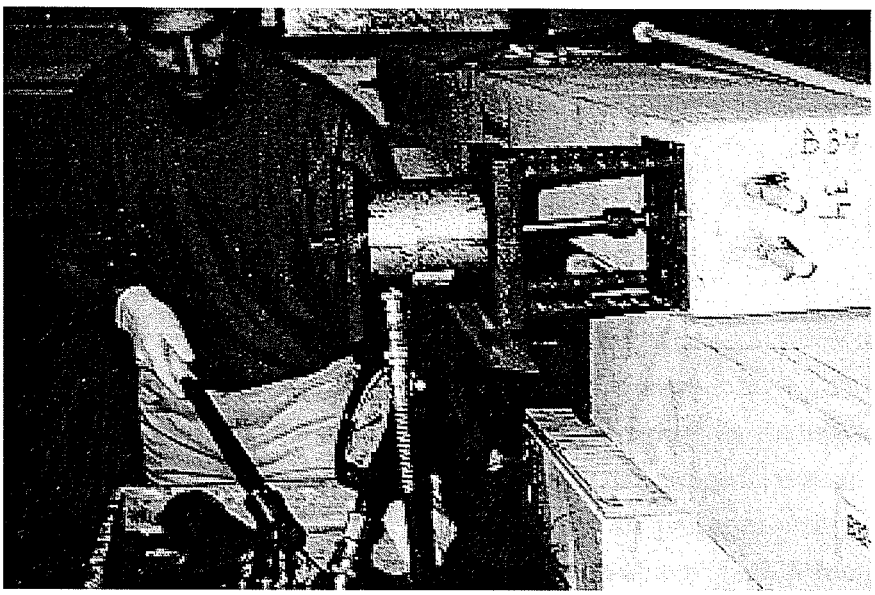

Figure 2.8 Loading Process [Kahhaleh, 1994].

In the previous study, the beams were subjected to a 3.5 percent NaCl solution flowing over the beam surfaces within a defined exposure area (area of exposure was controlled using dikes, see dark area in Figure 2.6) for 3 days followed by a dry period of 11 days. Periodic wetting and drying was imposed to ensure continuous transport of corrosive substances to steel surfaces to promote corrosion. The cracked beams were loaded and unloaded five times in a short period during each wetting and drying period. Each time the load reached a level that produced the desired maximum crack width.

2.2.3 Monitoring

The beams were monitored by taking half-cell potential readings according to ASTM C876-87 [1987] throughout the four and a half year duration of the project. A schematic of the half-cell potential circuit is shown in Figure 2.9. The readings for longitudinal bars and stirrups inside the concrete were taken periodically against a saturated calomel reference electrode (SCE). The readings were taken along the bars every 6 in. for longitudinal reinforcement and 2 to 4 in. for the stirrups in order to detect any localized corrosion in the bars. Points of half-cell potential measurements are shown in Figure 2.10.

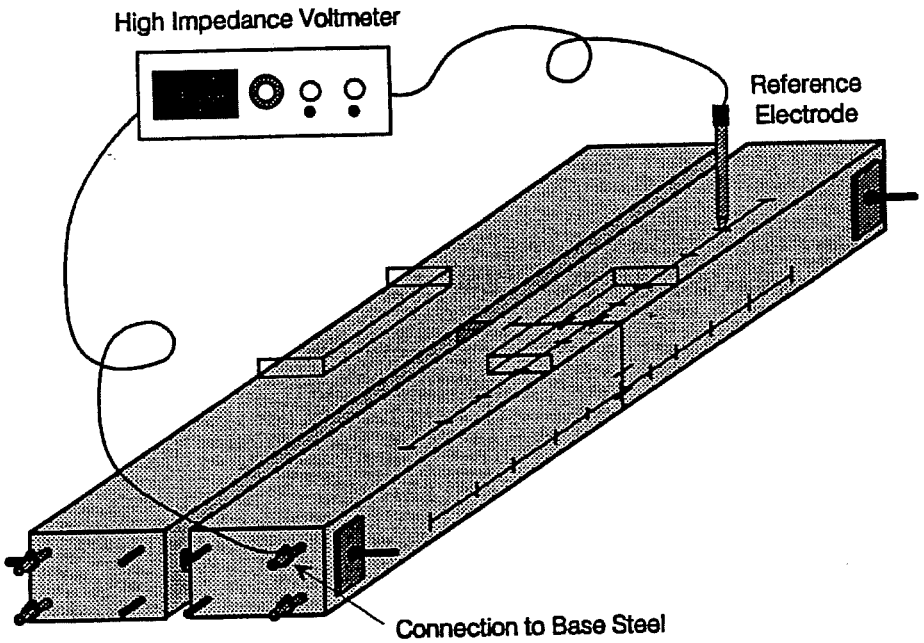

Figure 2.9 Schematic Diagram of Half-Cell Measuring Circuit [Kahhaleh, 1994].

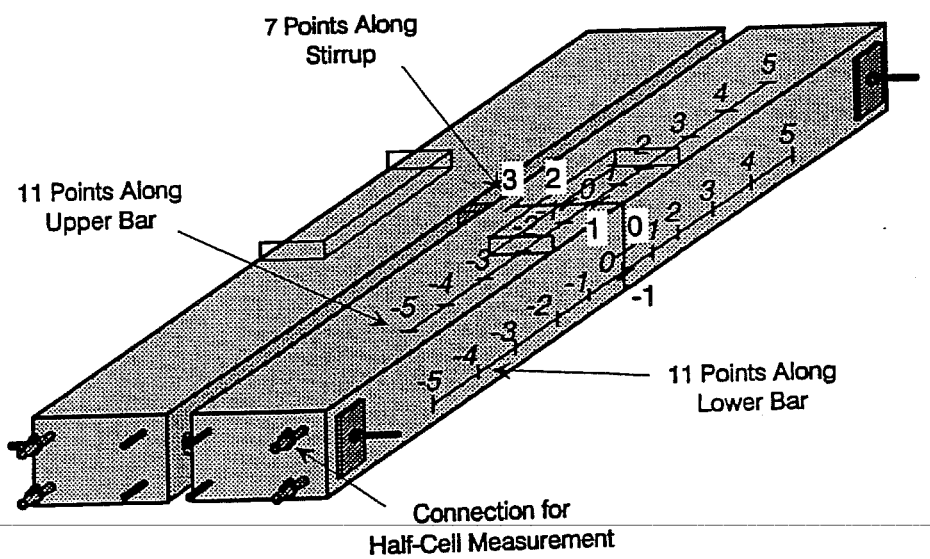

Figure 2.10 Points of Half-Cell Measurement [Kahhaleh, 1994].

2.2.4 Half-Cell Potentials

The half-cell potential readings (mV. vs. SCE) versus the time of exposure throughout the duration of the previous study are shown in Figures 2.11 through 2.16. In the graphs, black bar denotes the uncoated bar, epoxy 1 is the "upper" epoxy-coated bar when the beams are in exposure position (on their side), and epoxy 2 is the "lower" epoxy-coated bar in the exposure position (Figure 2.6). Monitoring of the black bars began about 18 months after the study started.

According to ASTM C876-87 [1987] "half-cell potentials demonstrate the thermodynamic behavior of reinforcing steel in concrete". The probability of corrosion of uncoated steel in concrete is determined by the empirical half-cell potential criteria shown in Table 2.2.

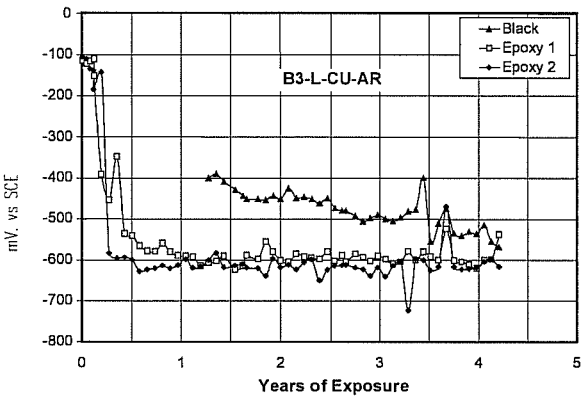

Figure 2.11 Half-Cell Potential Readings for Beam 3.

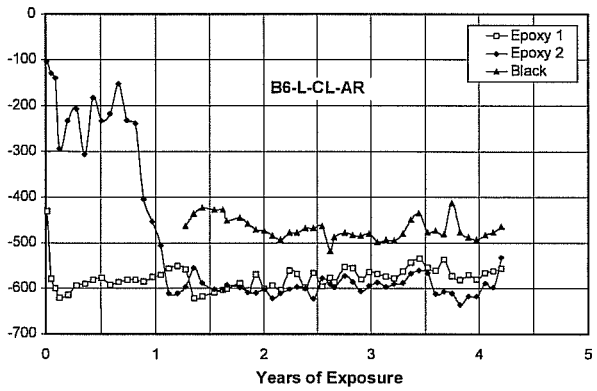

Figure 2.12 Half-Cell Potential Readings for Beam 6.

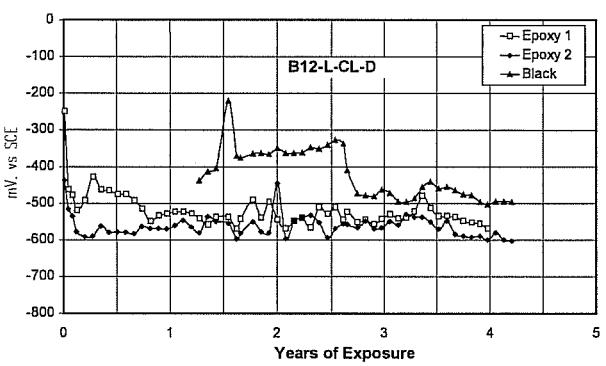

Figure 2.13 Half-Cell Potential Readings for Beam 12.

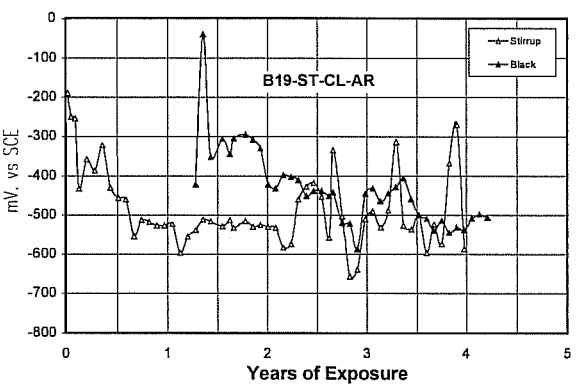

Figure 2.14 Half-Cell Potential Readings for Beam 19.

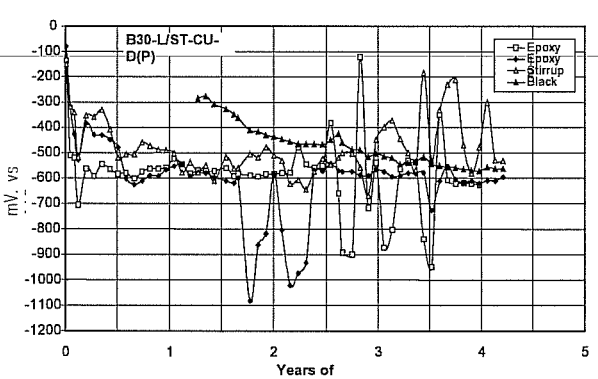

Figure 2.15 Half-Cell Potential Readings for Beam 30.

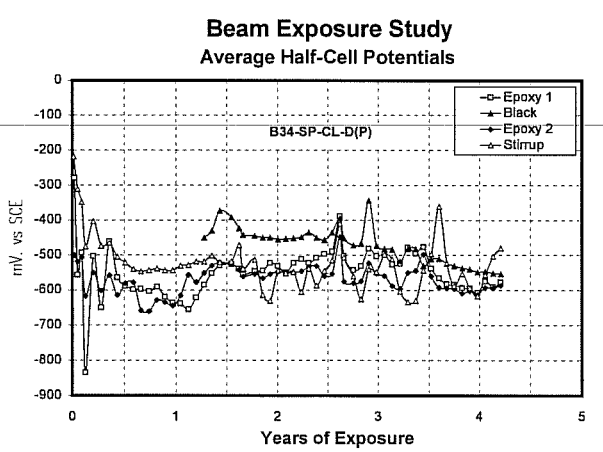

Figure 2.16 Half-Cell Potential Readings for Beam 34.

Table 2.2 Interpretation of Half-Cell Potentials Based on ASTM C876-87.

Probability of Corrosion	Half-Cell Potential Reference	
	Copper/Copper Sulfate, CSE (mV)	Saturated Calomel, SCE (mV)
Less than 10% if potential is less negative than	-200	-125
More than 90% if potential is more negative than	-350	-275
Uncertain if potential is between	-200 and -350	-125 and -275

2.2.5 Chloride Contents

In addition to half-cell potential measurements, the chloride content was measured at the end of the study. The readings ranged from 0.46 percent to 1.07 percent [Vaca, 1998] and are discussed in detail in Chapter 5.

2.3 Macro-Cells

2.3.1 Properties

The macro-cells are concrete prisms that were designed to simulate the conditions of a bridge deck slab exposed to deicing salt. The beams had a 148 mm. (6 in.) by 300 mm. (12 in.) cross section and were 225 mm. (9 in.) long. A bent, epoxy-coated 25-mm. bar was located near the top and three straight 28-mm. bars near the bottom. Cross sections of macro-cell specimens are shown in Figure 2.17.

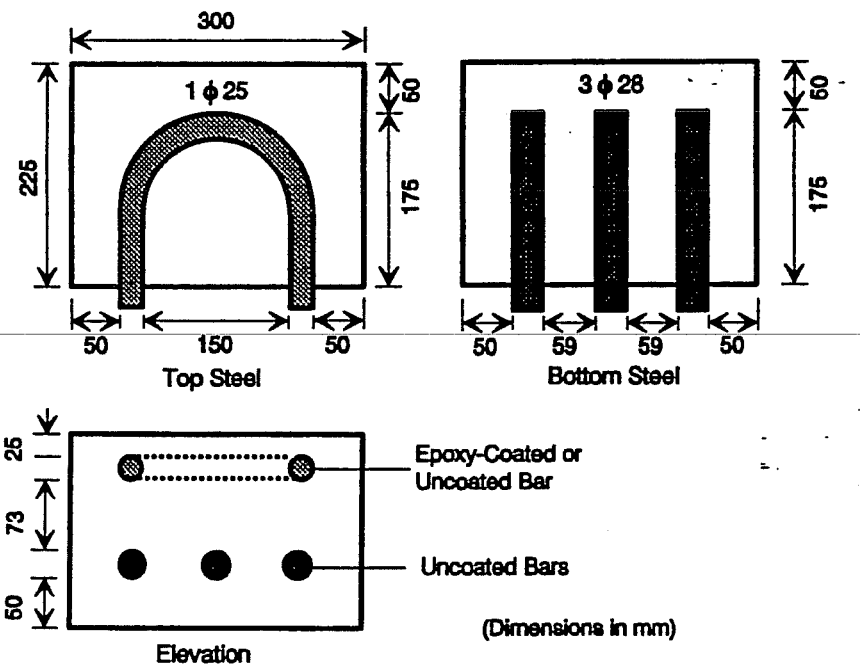

Figure 2.17 Details of Series B Macro-Cell Specimen [Kahhaleh, 1994].

There were several different groups of macro-cells where different parameters such as deformation pattern of ribs, epoxy-coating damage levels, and damage conditions were considered. Types of macro-cell specimens used for the encapsulation program were all B Series macro-cells which contained bars with cross ribs while the A Series macro-cells had bars with parallel ribs. The summary of damage to bars in the Series B macro-cells used in the encapsulation study are given in Table 2.3.

Table 2.3 Summary of Macro-Cell Bar Damage [Vaca, 1998].

Specimen - Type	Epoxy Coating Damage Level		Damage Condition	
	Spots > 6x6 mm	Pinholes < 1%	Patched	Not Patched
1B8 – Encapsulated	Control Specimen - Uncoated Bars			
1B* - Encapsulated	Additional Specimen - Very Thin Coating			
3B9 – Control	●		●	
2B10 –	●			●
2B11 – Control		●		●

All macro-cells had the same concrete properties. The concrete compressive strength-time curve is shown in Figure 2.18.

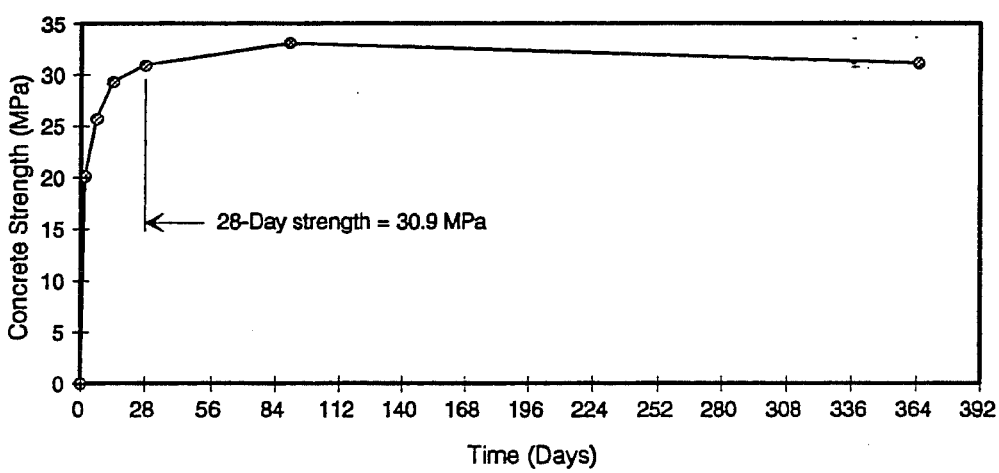

Figure 2.18 Concrete Strength-Time Curve for Macro-Cell [Kahhaleh, 1994].

2.3.2 Test Setup

To simulate the conditions of a bridge deck exposed to salt solution, a 3.5 percent NaCl solution was ponded on the top surfaces for 2 weeks followed by a 2-week dry period. The solution was removed during the dry period. Plexiglass dikes 75 mm. (3 in.) high were mounted with silicon to contain the salt solution. A schematic of the specimens is shown in Figure 2.19. The specimens were placed on narrow wooden strips to allow air circulation under the soffits. Plywood was placed on top of the dikes in order to prevent evaporation.

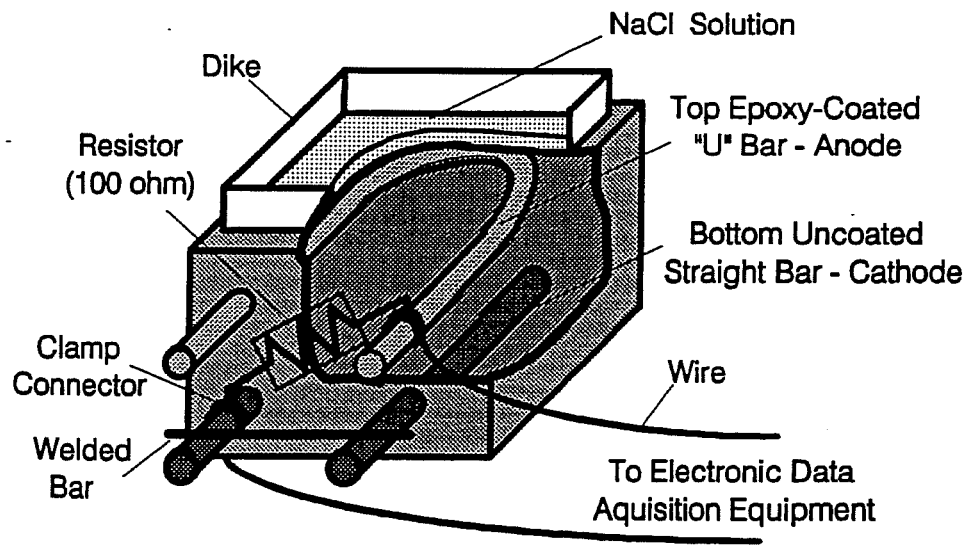

Figure 2.19 Macro-Cell Specimen Schematic [Kahhaleh, 1994].

2.3.3 Monitoring

Top and bottom layers of bars were linked using a 100-ohm resistor. The voltage drop across the resistor was measured periodically and the voltage was converted to current using Ohm's Law.

2.3.4 Corrosion Currents

Macro-cell potential readings were converted to current using Ohm's Law. The current was plotted versus the time of exposure for the duration of the previous study as shown in Figure 2.20 through 2.24. The short-term oscillations in the curve reflect the beginning and end of each wet and dry period.

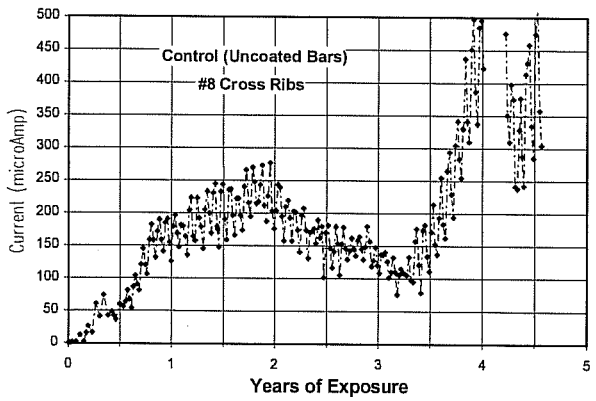

Figure 2.20 Macro-Cell Corrosion Currents, Specimen 1B8.

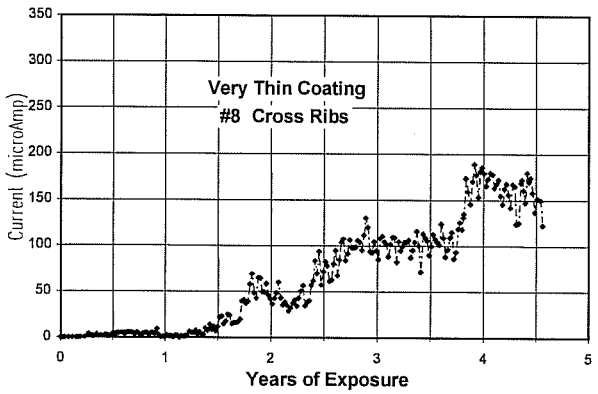

Figure 2.21 Macro-Cell Corrosion Currents, Specimen 1B.*

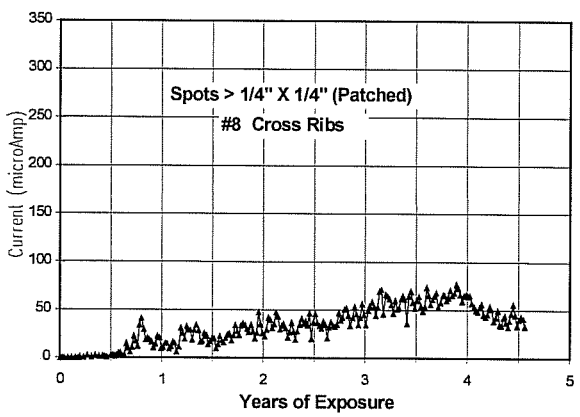

Figure 2.22 Macro-Cell Corrosion Current, Specimen 3B9.

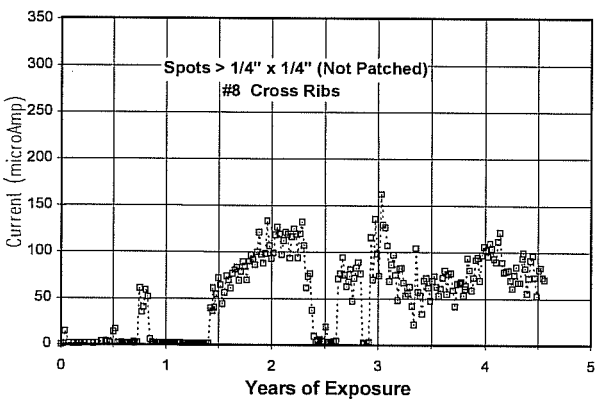

Figure 2.23 Macro-Cell Corrosion Currents, Specimen 2B10.

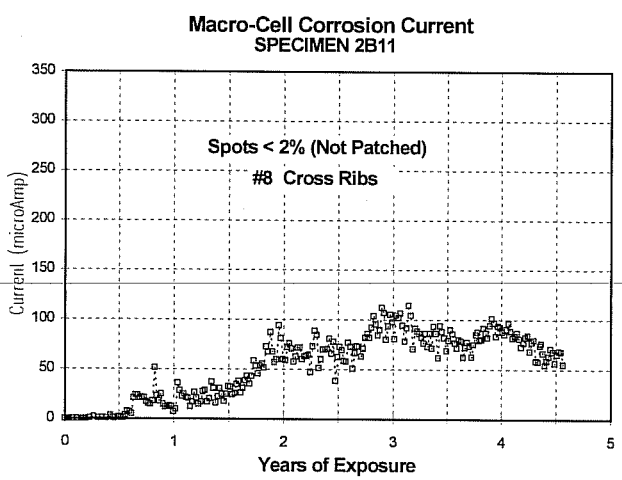

Figure 2.24 Macro-Cell Corrosion Currents, Specimen 2B11.

2.3.5 Chloride Contents

Chloride contents were measured at the end of the study. The readings ranged from 0.20 percent to 0.38 percent [Vaca, 1998] and are discussed in detail in Chapter 5.

CHAPTER 3

ENCAPSULATION AND EPOXY INJECTION PROCESS

3.1 ENCAPSULATION AND EPOXY INJECTION OF BEAMS

The encapsulation and epoxy injection of beams was performed in a ten step Hardshell-CSRS Process. Properties of the materials are given in Appendix A.

3.1.1 Plate And Angle Fabrication

The plates and angles, which were E-glass fiber reinforced composites, were prefabricated in a controlled facility using the SCRIMP (Seemann Composites Resin Infusion Molding Process) vacuum infusion process. Installation time was reduced by pre-measuring the structure for exact cutting dimensions. Cutting composite segments in the shop eliminated on-site fitting.

Plates and angles were sandblasted for better adhesion and felt stripping was attached to one side (Figure 3.1). The felt was used to create a space between concrete surface and the shell and served as a bond line or channel for the adhesive to flow over the entire element. The felt stripping was laid out in specific patterns designed to promote or inhibit flow to specific areas.

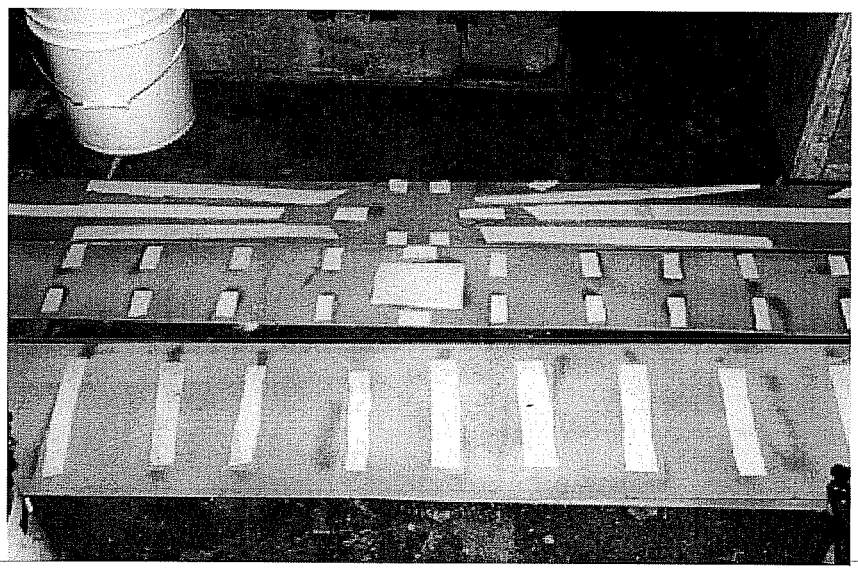

Figure 3.1 Felt Strips Attached on Side, Top, and Bottom Plates.

3.1.2 Concrete Surface Preparation

The concrete surface was prepared by pressure washing or grit blasting in order to provide a suitable surface for the adhesive system (Figure 3.2). The new material does not bond to the existing concrete surface unless the laitance produced by fine particles which may be carried to the surface by bleed water is removed to create a clean, sound concrete surface.

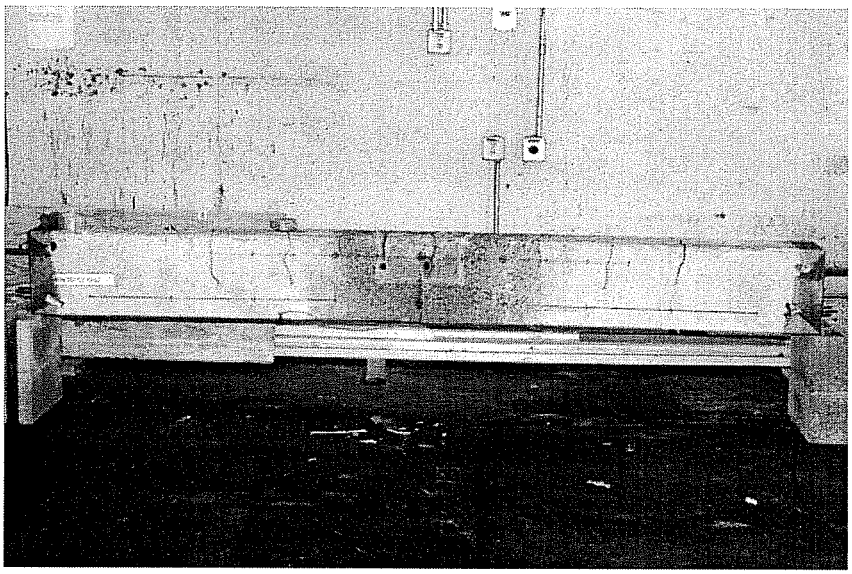

Figure 3.2 Beams Cleaned and Distribution Medium Placed at Ends.

3.1.3 Application of Distribution Medium

A distribution medium consisting of a coarse plastic mesh was applied at the ends of the beams in order to provide space for uniform epoxy flow in those regions where no composite panels were provided and where a plastic sheath was placed for developing a vacuum on the element (Figure 3.3).

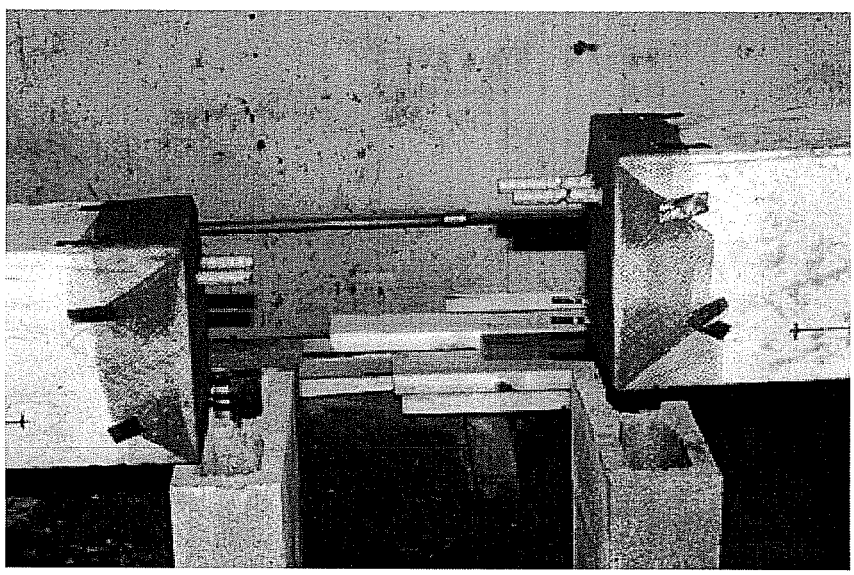

Figure 3.3 Application of Distribution Medium.

3.1.4 Plate And Angle Installation

The plates and angles were held together with a quick dry adhesive in place against the concrete so that the waterproofing (vacuum) membrane or plastic sheath could be applied and the resin injected.

Plates were erected in groups of opposing pairs (Figure 3.4) using quick dry adhesive, prefabricated wood jigs and pipe clamps to hold them in place (Figure 3.5). Angles were easily installed using the quick dry adhesive (Figure 3.6).

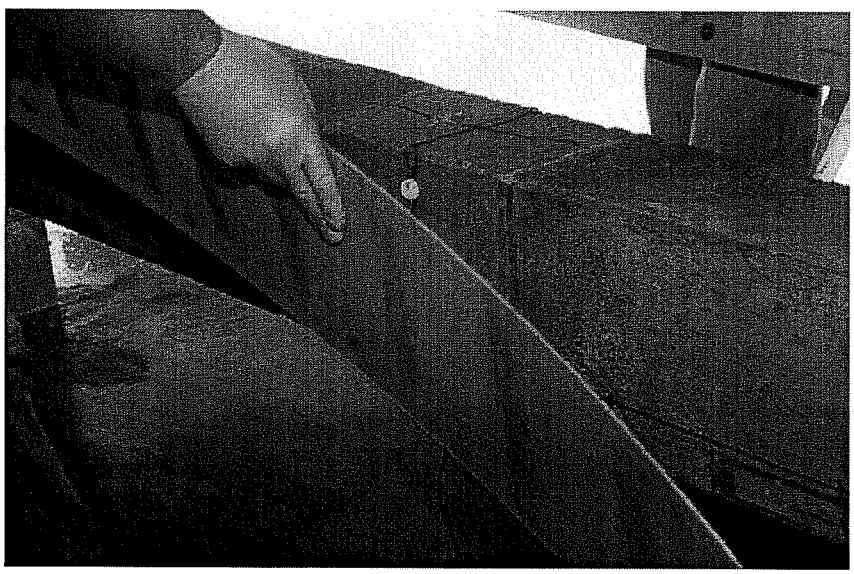

Figure 3.4 Erection of Plates.

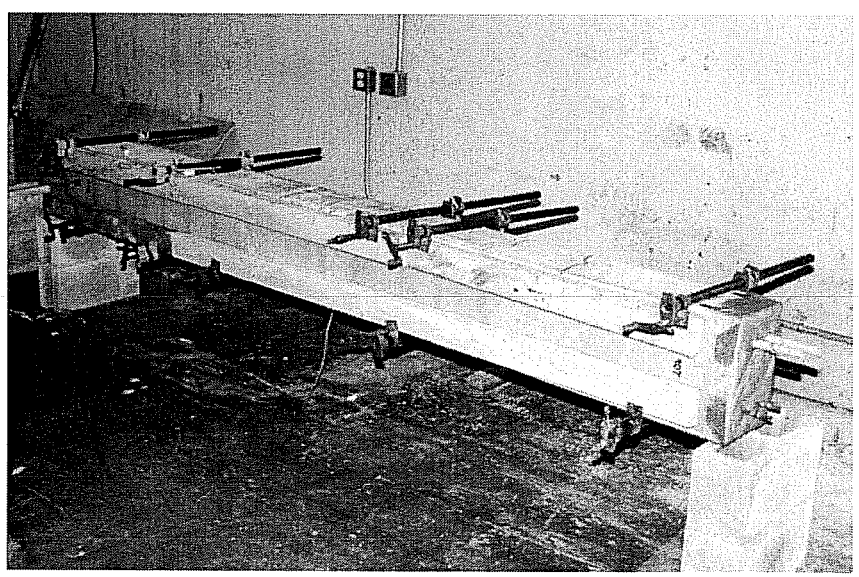

Figure 3.5 Wood Jigs and Pipe Clamps to Hold Composite Panels in Place.

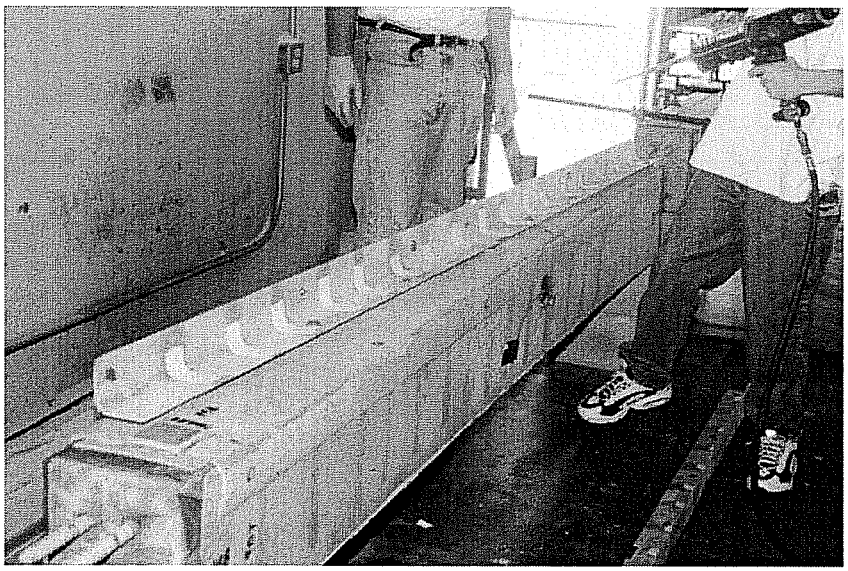

Figure 3.6 Installation of Angles.

3.1.5 Injection Ports

After the placement of plates and angles was completed, injection ports were installed on top and bottom of the beams for vacuum tube connections and for injecting resin (Figures 3.7, 3.8).

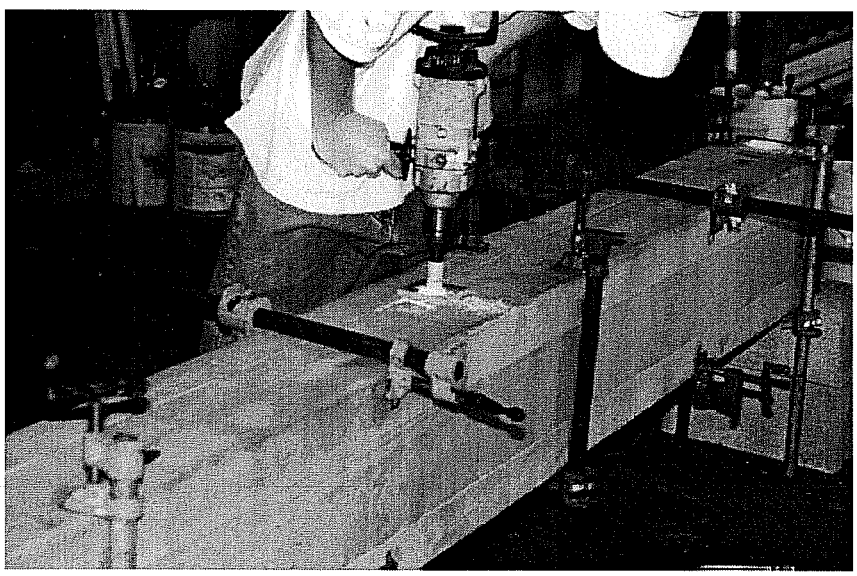

Figure 3.7 Installation of Injection Ports.

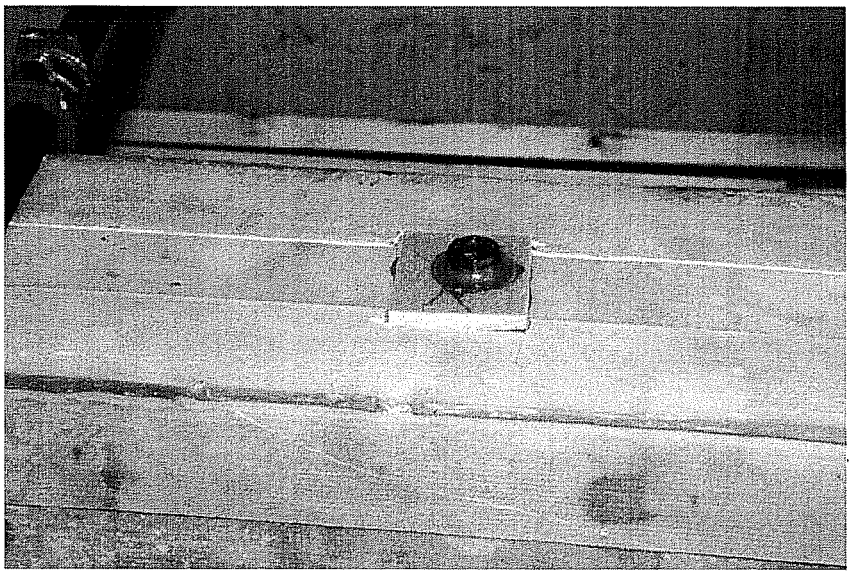

Figure 3.8 Installed Injection Port.

3.1.6 Airtight Membrane

In order to evacuate the member inside the shell, an airtight seal was placed over the plate and angle system. In the laboratory, plastic bags were used to provide a seal (Figure 3.9). The ends of the bags were sealed using special tape, which also served as a temporary patching material if a leak was found after evacuation started.

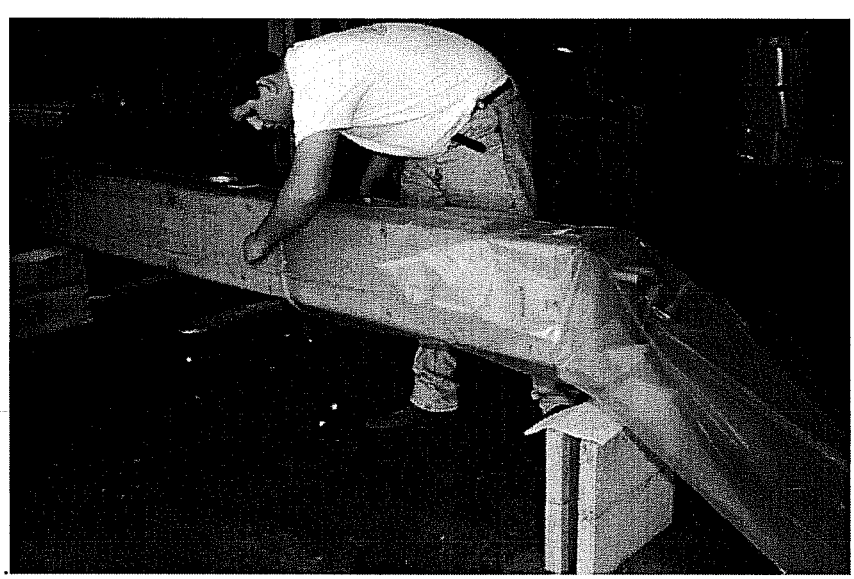

Figure 3.9 Application of Plastic Bags.

Under field conditions, an airtight seal would be provided using a spray methocrylate or polymer. The spray coating also provides a barrier that protects the composite wrapping against UV light and degradation.

3.1.7 Infusion Preparation

The encased and sealed concrete member was fitted with feeder inlets (Figure 3.10). The inlets were placed strategically to ensure quick and complete infusion of resin. The encapsulated element was then evacuated and a leak test was performed to check the integrity of the seal (Figure 3.11). Perfect vacuum was rarely achieved immediately after the vacuum was drawn. Leak checks were performed and leaks were sealed with temporary patching materials (Figure 3.12). These patches were removed following the infusion. The structure remained in a vacuum of 27 inches of mercury for 24 hours to remove excessive moisture in concrete. The system was then ready for infusion.

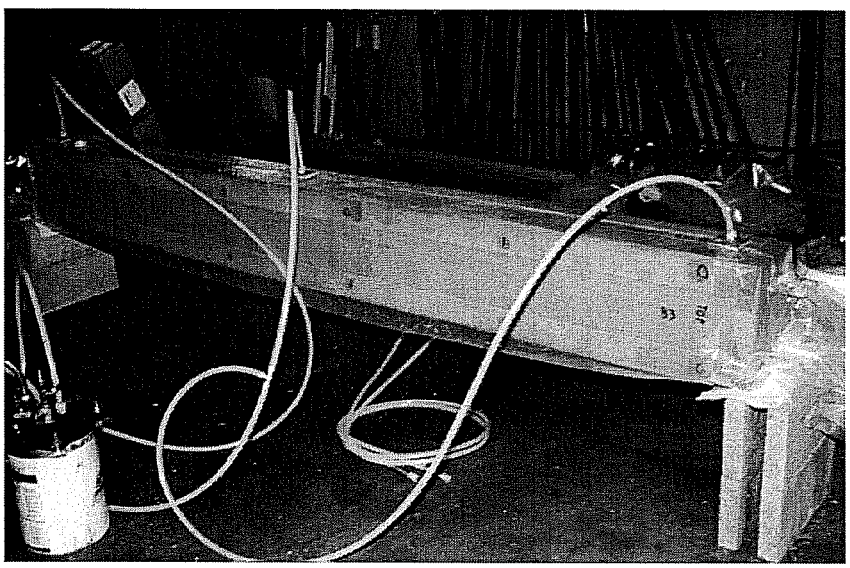

Figure 3.10 Feeder Inlets.

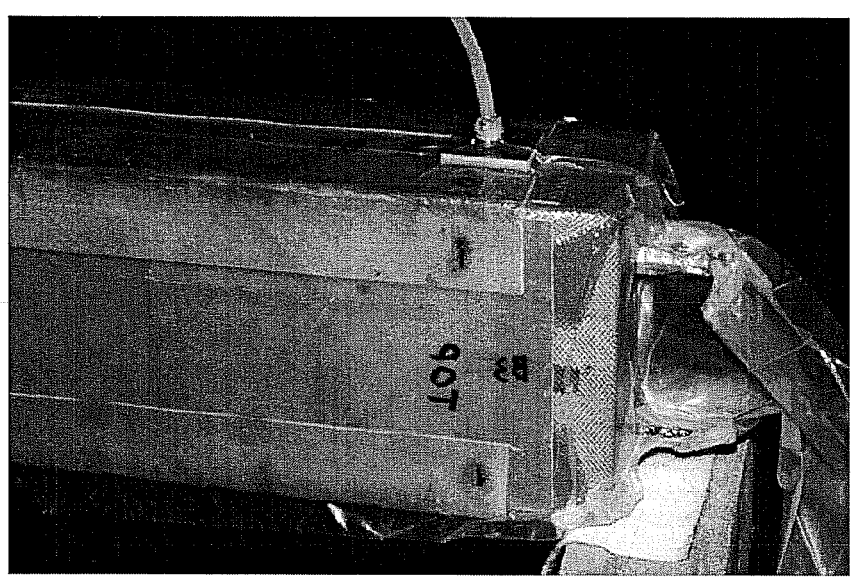

Figure 3.11 Evacuation Process.

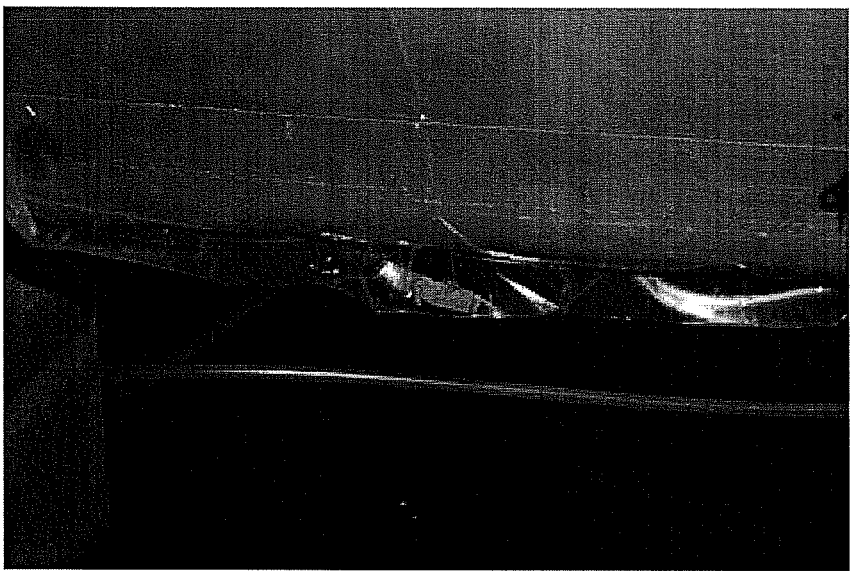

Figure 3.12 Using Tacky Tape as a Patching Material.

3.1.8 Mixing the Resin

Once the system was ready for infusion, the resin was mixed (Figure 3.13). Dow Derakane 8084 epoxy vinyl ester resin was used. Six percent cobalt napthenate was added to the resin at 0.4 percent by volume. After the cobalt napthenate was fully mixed with the resin, Trigonox 239A was added at 2 percent by volume and mixed. The additive concentrations were selected to produce the desired gel time for infusion.

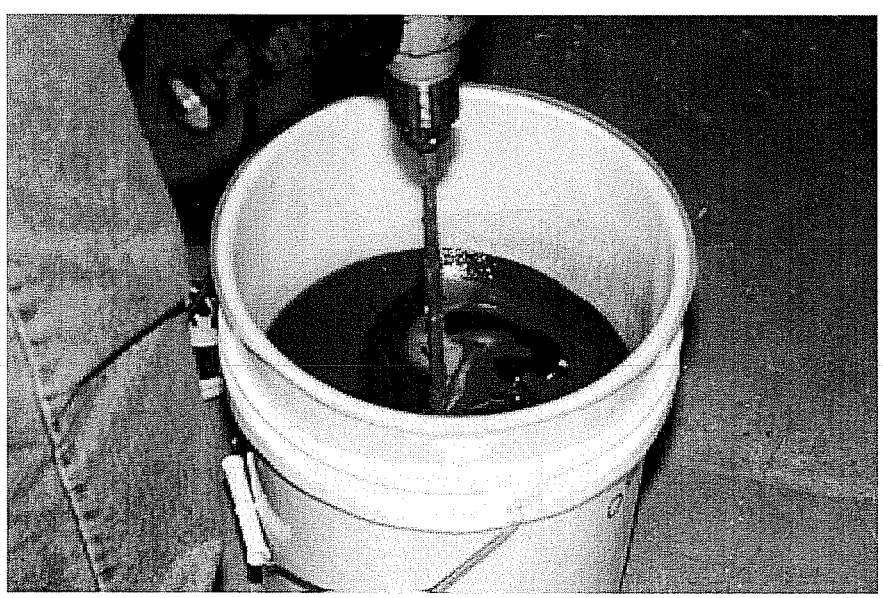

Figure 3.13 Mixing the Resin.

3.1.9 Infusion

The system was designed to draw resin from the bottom inlet ports, through the member, and out of the top vacuum ports (Figure 3.14).

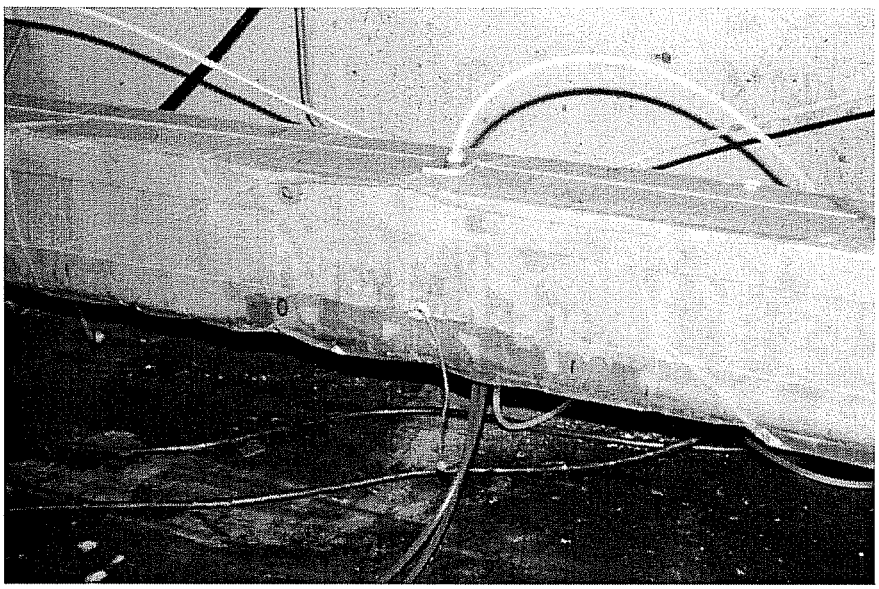

Figure 3.14 Epoxy Vinyl Ester Resin Infusion in Progress.

The felt strips directed the flow so that the entire structure was infused (Figure 3.15). Vacuum remained on the system for 24 hours until the adhesive reached specified mechanical properties (See Appendix B).

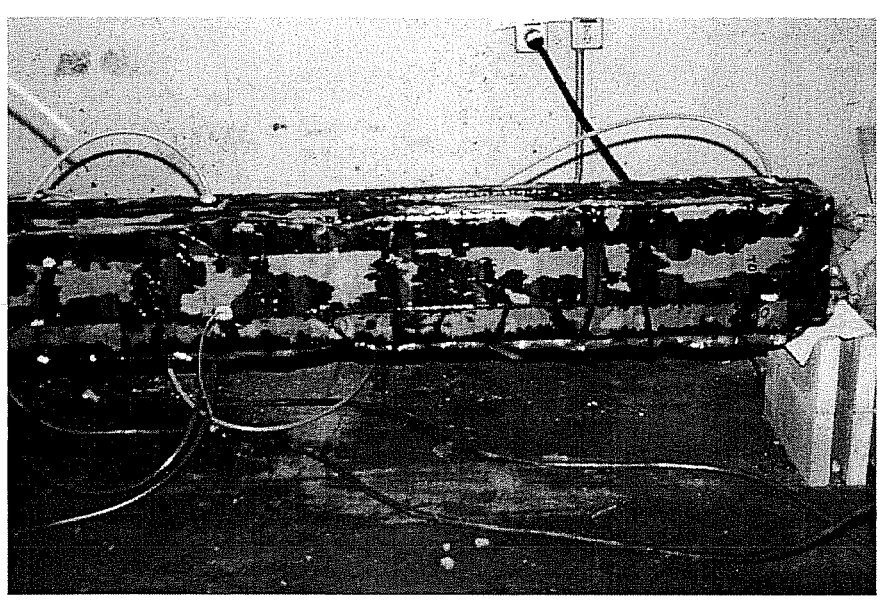

Figure 3.15 End of Encapsulation and Epoxy Injection Process.

3.1.10 Post Infusion Clean-up

In the field all the hoses would be removed following the 24-hour curing period. The port holes could be permanently patched as would temporary patches installed during the leak checks. A coating of methocrylate or polymer would then be sprayed on the patched areas to seal the surface and improve appearance. In the laboratory, all the hoses and plastic bags were removed after the 24-hour curing period.

3.2 Encapsulation and Epoxy Injection of Macro-Cells

The macro-cells were encapsulated and injected simultaneously with the beams. Since the macro-cells were small, no hardshell encapsulation was provided after the surface of the macro-cells was prepared as described in Section 3.1.2. The same distribution medium used for the beams was applied on all surfaces of the macro-cells in order to allow uniform resin flow beneath the plastic sheath (Figure 3.16).

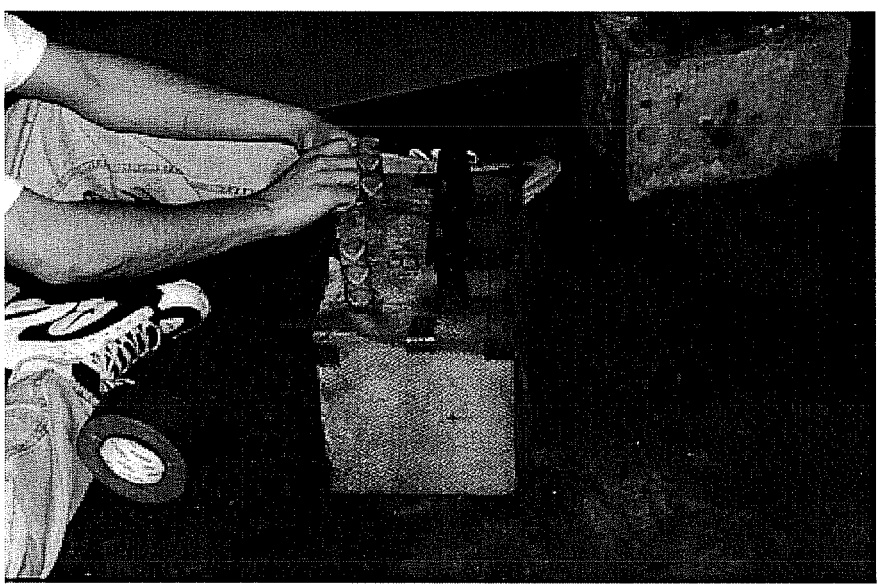

Figure 3.16 Application of Distribution Medium.

After the placement of the distribution media, injection ports were installed on the top and bottom faces of the macro-cells. Omega-shaped channels were used as injection ports (Figure 3.17). The macro-cells were placed in plastic bags and the ends of the bags were sealed (Figure 3.18).

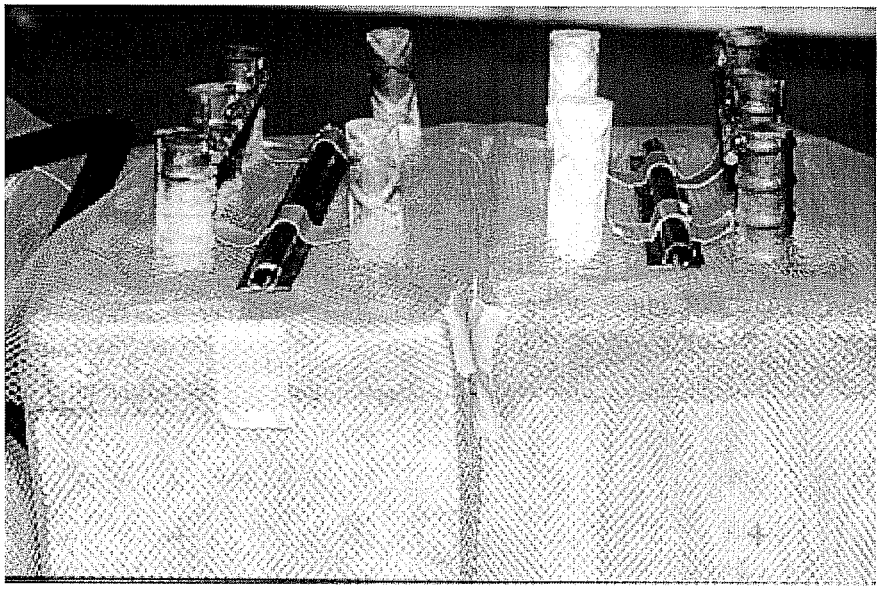

Figure 3.17 Application of Omega Channels as Injection Ports.

Figure 3.18 Application of Plastic Bags.

The feeder inlets were then installed (Figure 3.19). Leak checks were performed and all leaks were sealed with tackey tape. After 24 hours of evacuation at 27 inches of mercury, the resin was injected (Figures 3.20, 3.21 and 3.22). After a 24-hour curing period, all hoses were removed and the macro-cells were removed from the plastic bags (Figure 3.23).

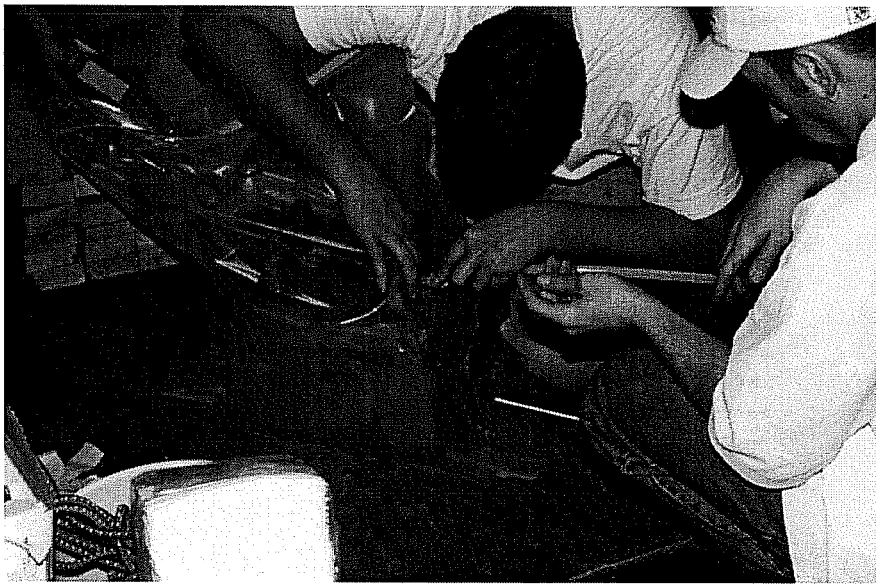

Figure 3.19 Application of Feeder Inlets.

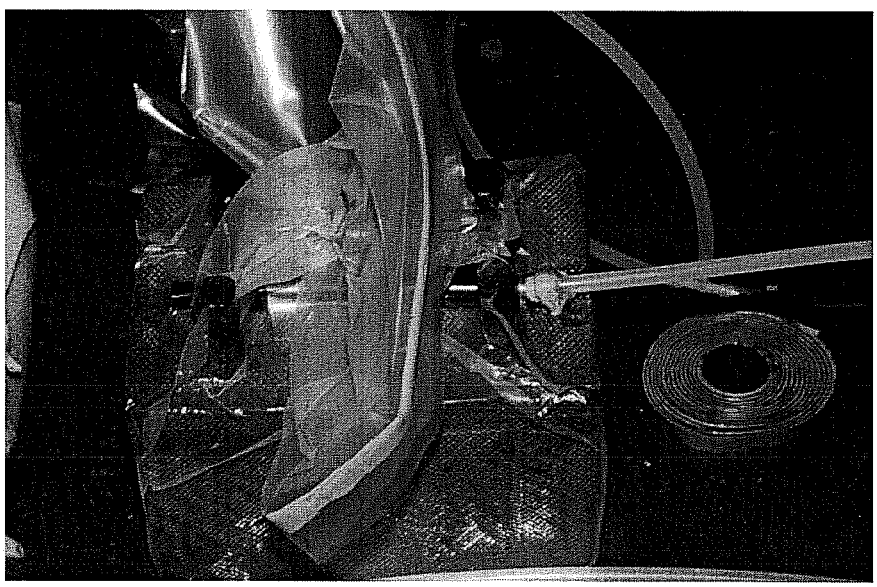

Figure 3.20 Evacuation Process.

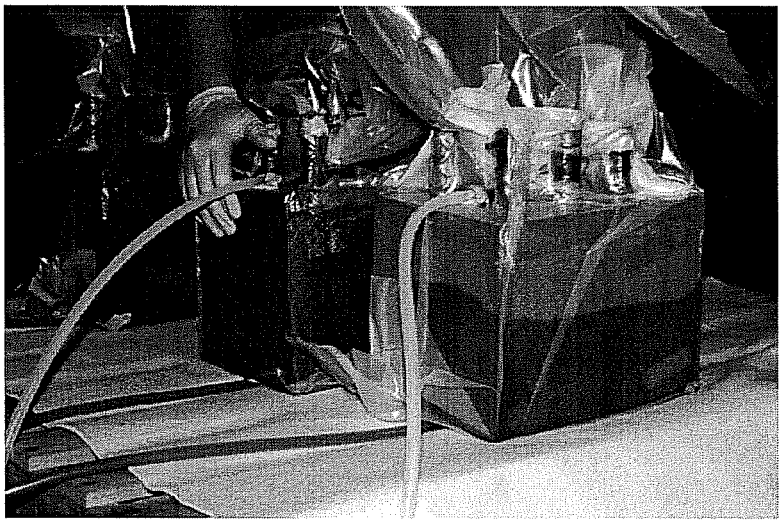

Figure 3.21 Epoxy Vinyl Ester Resin Injection in Progress.

Figure 3.22 End of Process.

Figure 3.23 Post Infusion Clean-up.

CHAPTER 4

TEST SETUP AND MONITORING

4.1 BEAM TESTS

4.1.1 Exposure and Test Setup

The beams were exposed to a 3.5 percent saline solution as in the previous study. The exposure time and the beam surface area exposed differed from that used in the previous study. Each exposure cycle consisted of a one week wet period followed by a 3-week dry period. Rather than exposing a defined area, the entire beam surface was exposed in order to assess the effectiveness of encapsulation. During the wet cycle, the corrosive solution was circulated over the beams continuously and then the beams were allowed to air dry for three weeks. Cloth was placed on the beams during the wet cycle in order to provide more uniform exposure over the entire beam since the corner plates of encapsulated beams formed a channel and prevented the solution from flowing over the sides of the beams (Figure 4.1). A total of thirteen 28-day exposure cycles were applied to the beams.

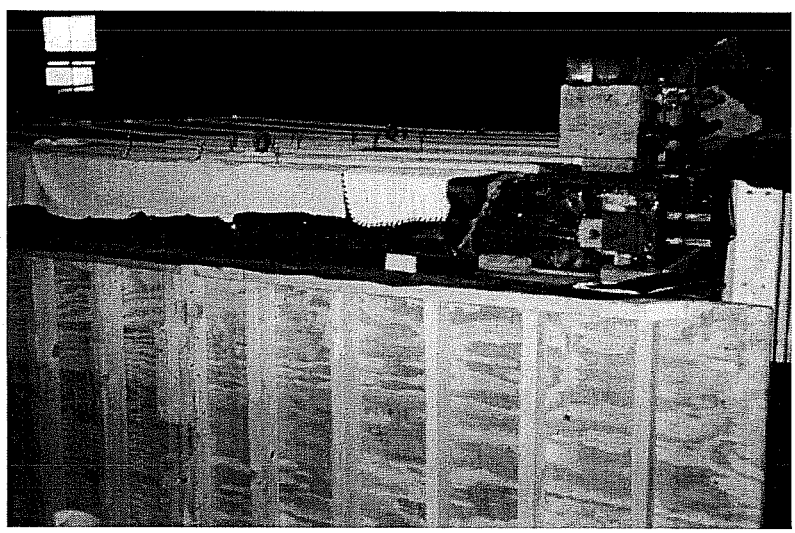

Figure 4.1 Cloth on Beams.

A retaining pool was built as shown in Figure 4.2. The retaining pool was fabricated using plywood sheets. A polyurethane sheet was placed to form the bottom of the pool and extended partially along the sides to form a catch basin for the solution. The remainder of the plywood side walls were covered with plastic sheets in order to protect the plywood. The pool was placed on an existing elevated slab. A drain in the base of the pool was connected to a pump that recirculated the water to the top of the beams through a distribution system of PVC pipes. Holes were drilled into the bottom of the PVC pipes to distribute the saline solution over the length of the beams.

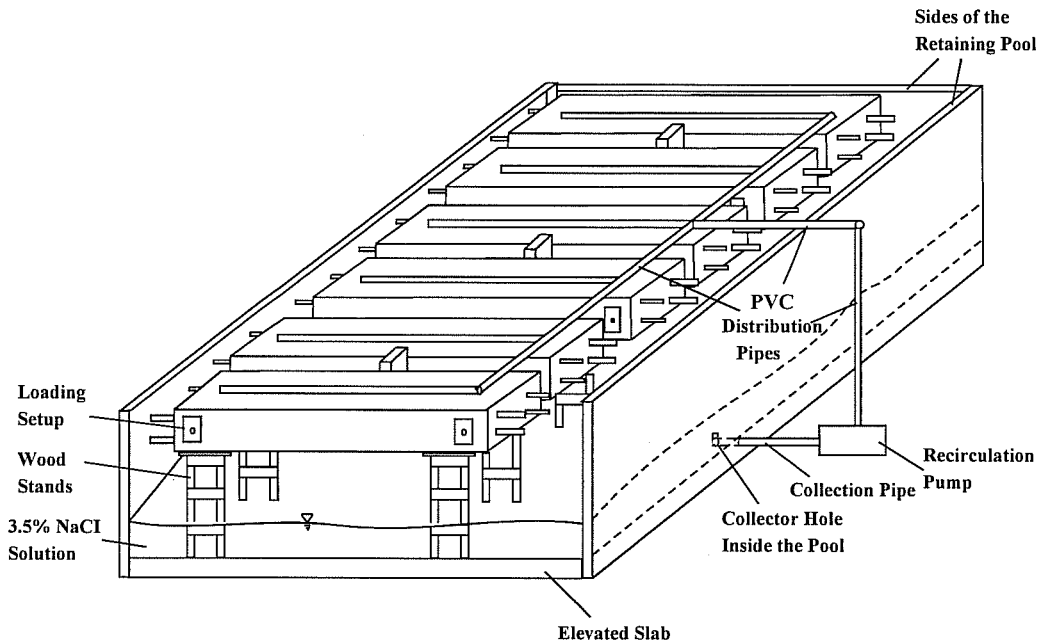

Figure 4.2 Test Setup for Beams.

The beams were placed on wood stands inside the pool to support them above the collected water. Figure 4.3 shows the placement of the beams on the stands. Figure 4.4 shows the retaining pool, the recirculation pump, and the PVC distribution pipes.

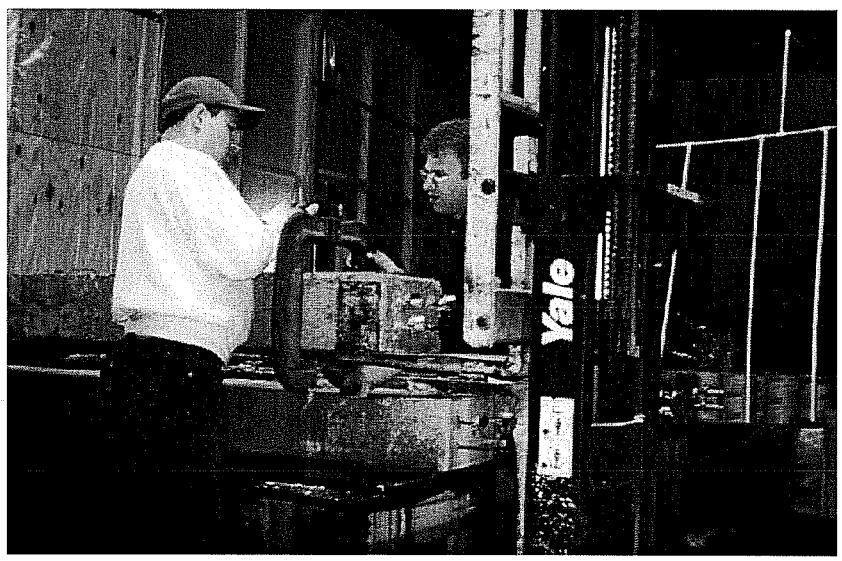

Figure 4.3 Placing the Beams on Wood Stands in the Retaining Pool.

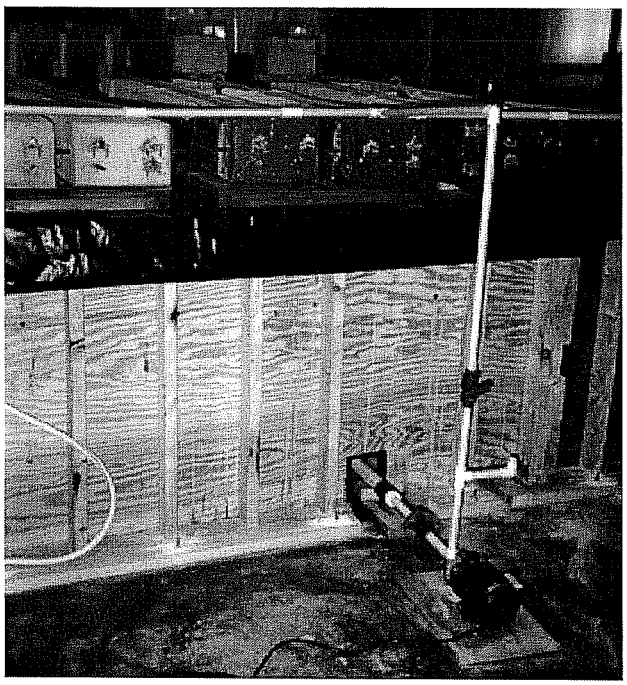

Figure 4.4 Retaining Pool, Recirculation Pump, and PVC Distribution Pipes.

4.1.2 Loading

Before the start of the exposure cycles, the encapsulated beams were loaded to reach two thirds of the yield stress in order to crack the concrete but below the level that would yield the bar. The beams were loaded back to back as simple beams with peak moment at the center. As a result, cracking was concentrated near the mid-span where the stirrup was located. The load-deflection plot is shown in Figure 4.5. The effectiveness of the encapsulation process was studied in the situation where loads on the structure are sufficient to crack the concrete.

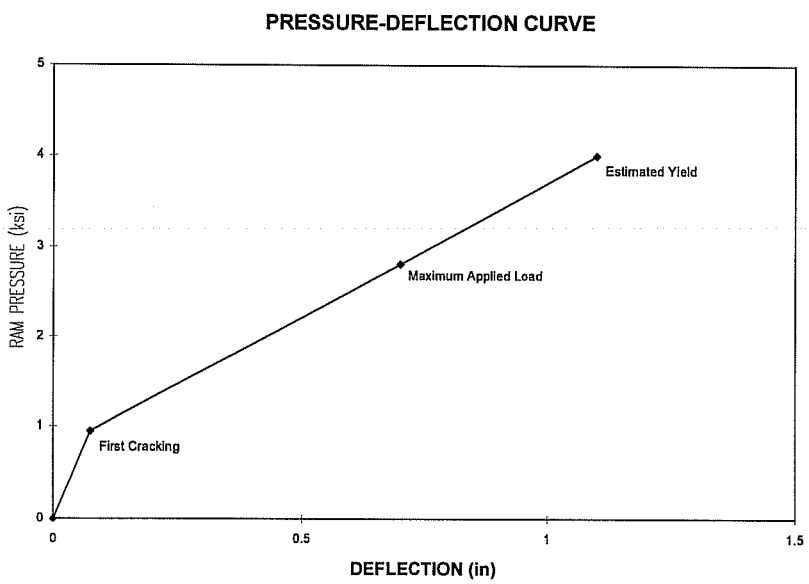

Figure 4.5 Beam Pressure-Deflection Prior to Exposure.

Once the exposure study started, four of the six beams (two encapsulated, two control beams) were loaded back to back, while two were not loaded. The loading setup can be seen in Figure 4.6. Once each week the four loaded beams were unloaded and reloaded 5 times. The last load was maintained to keep the cracks open (this was done in the previous study). Load levels were the same as in the previous study.

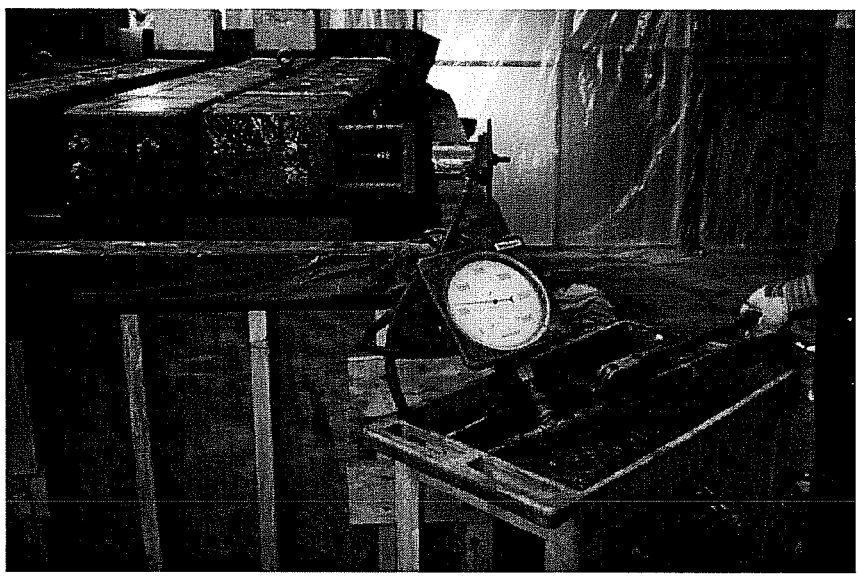

Figure 4.6 The Loading Process.

4.1.3 Monitoring

For one year, half-cell potential readings against a saturated calomel reference electrode (SCE) were taken. The readings were taken weekly for the control specimens and every 3 months for the encapsulated ones. The 3-month intervals were selected so that the composite shell on the encapsulated beams would not be disturbed. Figures 4.7 and 4.8 show the procedure for taking half-cell potential readings for unencapsulated and encapsulated beams respectively. For the encapsulated beams, a number of access holes through the fiber composite were provided along the beams at the level of the bars in order to access the concrete surface for half-cell potential measurements. The holes were limited in number in order to avoid disturbing the continuity of the encapsulated beams. Figure 4.9 shows the access holes on encapsulated beams. After taking the readings, the access holes were sealed using silicon. When the access holes were opened in order to take the readings a clear fluid was found inside the holes. The fluid was collected and analyzed; the results are discussed in Chapter 5. For the control specimens, readings were continued on a weekly basis since the surface could be accessed at the same locations as in the previous study.

In addition to half-cell potential measurements, acoustic emission testing was performed on the beams in order to determine the applicability of that technique for corrosion monitoring. The acoustic emission application is discussed in Appendix B.

Figure 4.7 Macro-Cell Readings–Unencapsulated Beams.

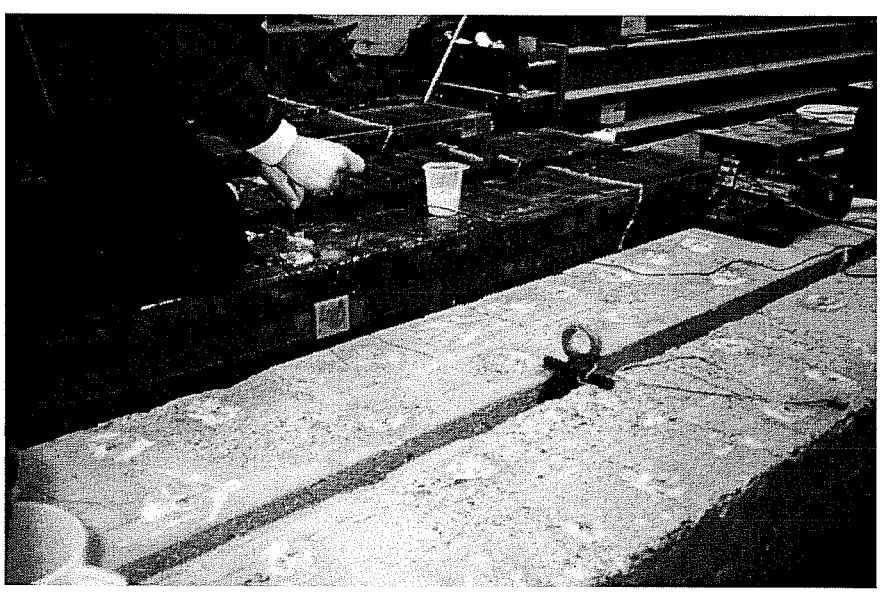

Figure 4.8 Macro-Cell Readings–Encapsulated Beams.

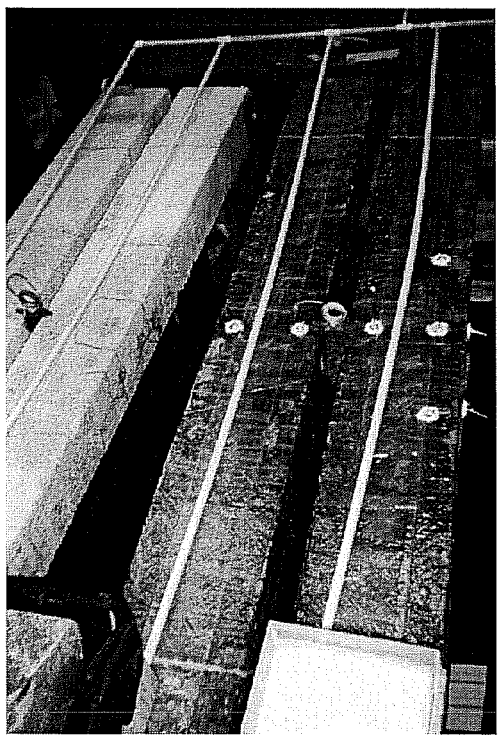

Figure 4.9 Access Holes on Encapsulated Beams.

At the end of the exposure period, core samples were taken from the encapsulated beams to assess the depth of resin impregnation (Figure 4.10). The beams were autopsied to assess the condition of the bars and the concrete around the bars. Finally, the bars were removed from concrete. The results from the half-cell potential monitoring and the autopsies are discussed in Chapter 5.

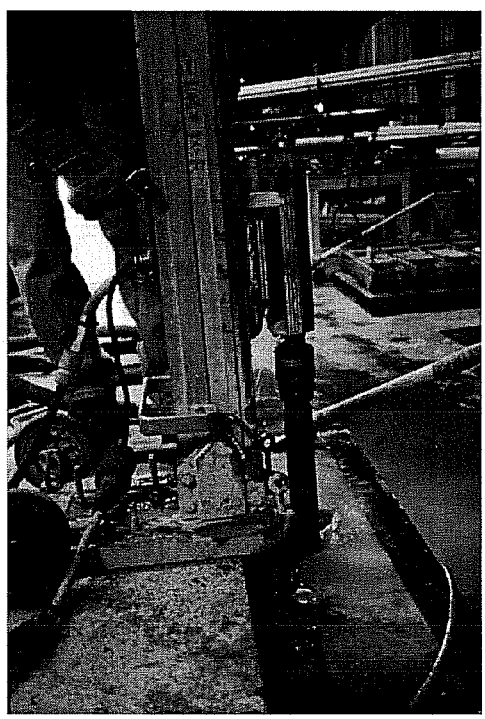

Figure 4.10 Taking Core Samples from Beams.

4.2 MACRO-CELL TESTS

4.2.1 Exposure and Test Setup

The macro-cells were exposed to a 3.5 percent by weight NaCl solution. For the macro-cells, the exposure cycles consisted of a 2-week wet period followed by a 2-week dry period. The same exposure cycle was used in the previous study. The test setup for the encapsulated macro-cells was modified to better evaluate the effectiveness of the resin encapsulation procedure. During the wet period, the encapsulated macro-cells were placed upside down inside a small retaining pool that had a slanted base (30° angle with the horizontal), and the pool was filled with the saline solution. When the wet period ended, the specimens were taken out of the water. By placing the specimen in the water rather than placing a small dike at the top surface and filling it with the saline solution, the face and part of the sides (including the corners, which are harder to seal) are exposed. The control specimens were ponded just as they had been in the previous study. Thirteen exposure cycles were applied. Figure 4.11 shows the retaining pool and the test setup for the encapsulated macro-cells and Figure 4.12 shows the test orientation both encapsulated and control macro-cells.

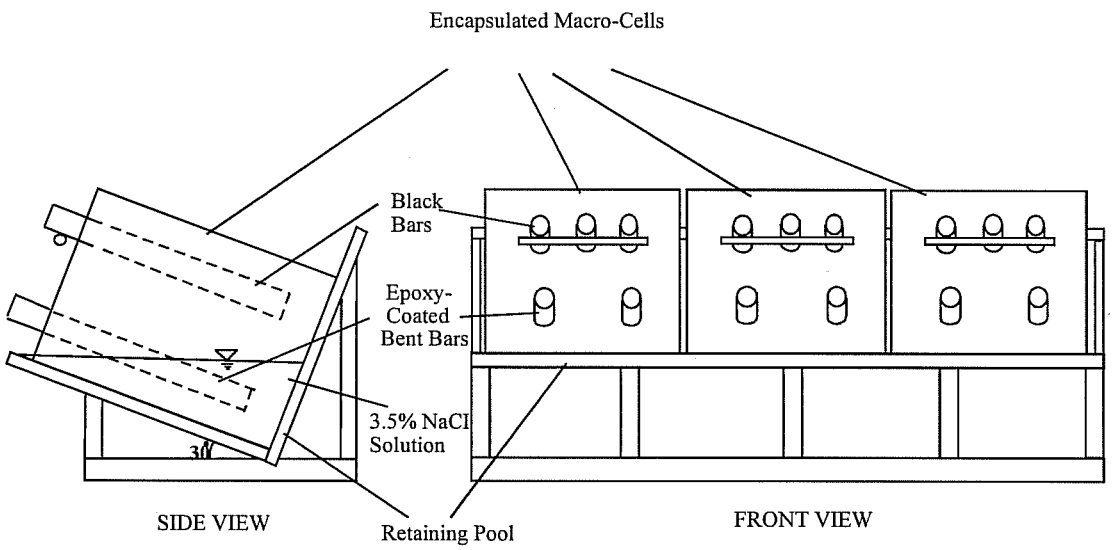

Figure 4.11 Retaining Pool and Test Setup for Encapsulated Macro-Cells.

Figure 4.12 Orientation of Macro-Cells During Exposure.

4.2.2 Monitoring

Potential readings were taken twice a week. Top and bottom reinforcing layers were linked using a 100-ohm resistor. The voltage drop across the resistor was measured with a voltmeter and the voltage was converted to current using Ohm's Law.

In addition to macro-cell potential readings, the control specimens were monitored by taking half-cell potential readings against SCE each week. This could not be done for the encapsulated macro-cells since there was no access to the concrete surface.

At the end of the exposure cycles, the macro-cells were opened to assess the condition of the bars and the concrete, and the penetration of the resin. Finally, the bars were removed from concrete. The results from the monitoring processes and the autopsies are discussed in Chapter 5.

CHAPTER 5

TEST RESULTS AND DISCUSSION

5.1 BEAMS

5.1.1 Half-Cell Potentials

The half-cell potentials for the duration of the encapsulation study as well as the previous study are shown in Figure 5.1 through 5.6. The previous study is shown as the TxDOT Program and the encapsulation study is shown as Encap. Program. There was a gap of 6 months between the two studies as shown. As described in Chapter 2, black bar refers to the uncoated bar, epoxy 1 to the "upper" epoxy-coated bar when the beams are in their exposure position (supported on a side face), and epoxy 2 to the "lower" epoxy-coated bar in the exposure position (Figure 2.6).

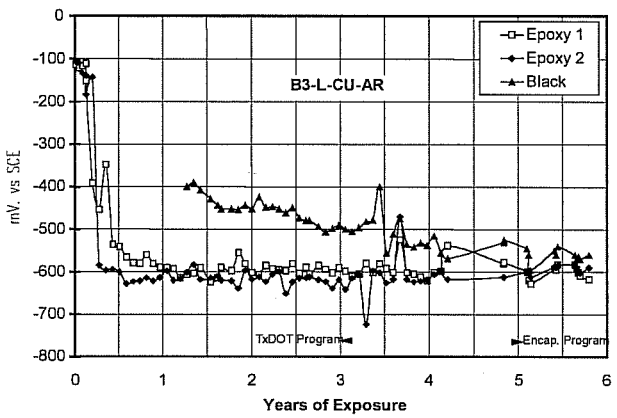

Figure 5.1 Half-Cell Potential Readings for Beam 3.

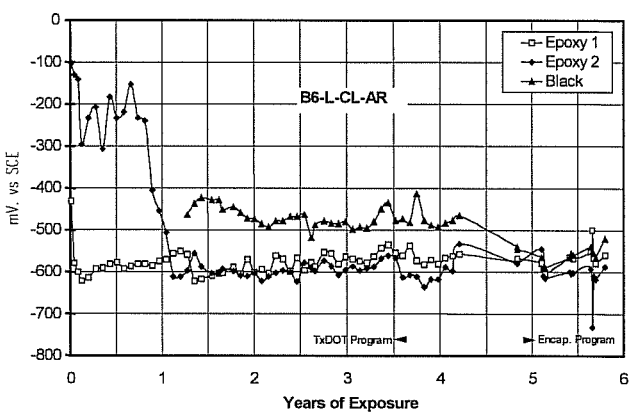

Figure 5.2 Half-Cell Potential Readings for Beam 6.

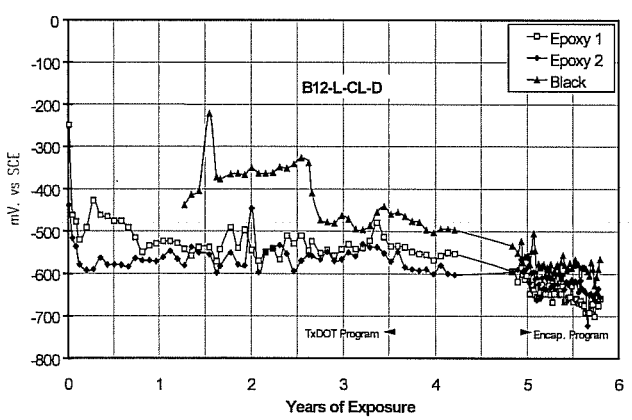

Figure 5.3 Half-Cell Potential Readings for Beam 12 (Control).

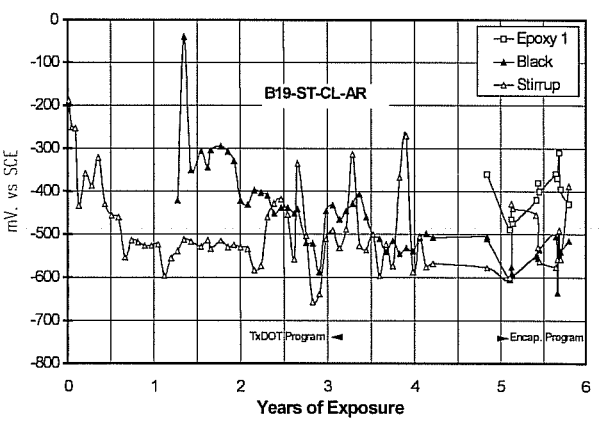

Figure 5.4 Half-Cell Potential Readings For Beam 19.

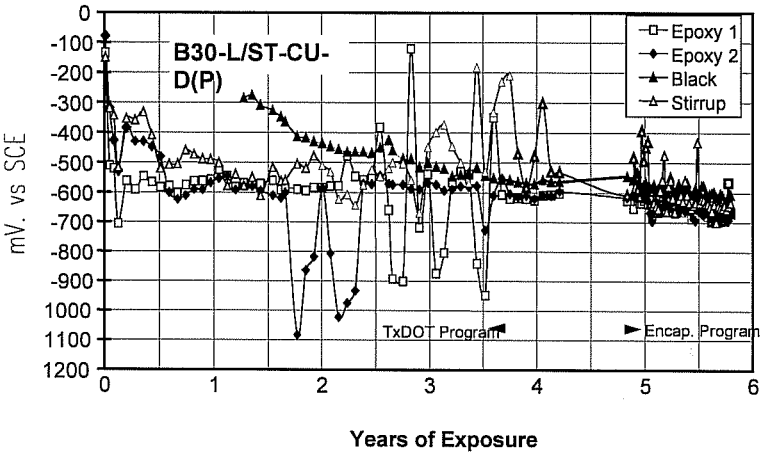

Figure 5.5 Half-Cell Potential Readings for Beam 30 (Control).

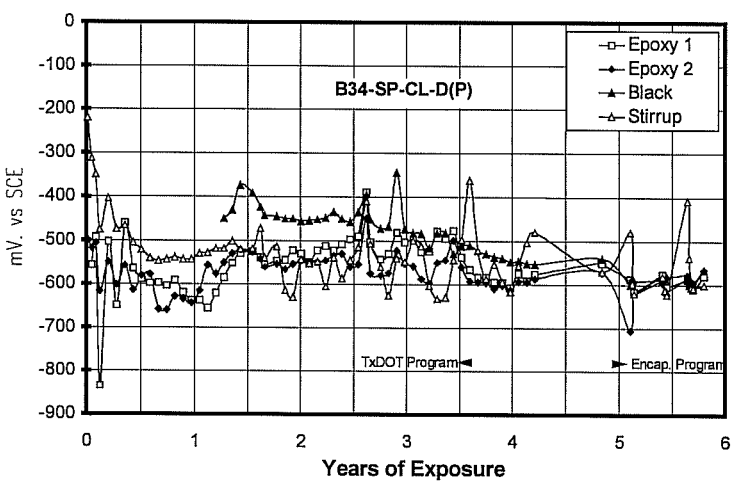

Figure 5.6 Half-Cell Potential Readings for Beam 34.

Readings for the encapsulated and control specimens remained at nearly the same level they were when the previous study ended. With the readings remaining at the same level it is evident that the evacuation procedure did not remove moisture from the encapsulated specimens and that there was sufficient moisture, oxygen, and chlorides in the specimens within the composite shell to allow corrosion to continue.

The half-cell potential readings indicate a 90 percent or higher probability of corrosion according to the interpretation in Chapter 2. However, there is not always a direct correlation between the half-cell potential readings and the amount of corrosion damage inside the beams as found in the previous study. That is, corrosion in a beam showing more negative values is not necessarily worse than corrosion in a beam showing less negative values if both readings are above a certain threshold (-275 mV.) [Vaca, 1998].

The fluid found in the access holes of the encapsulated specimens (described in Chapter 4) was analyzed using Mass Spectrometry. The results indicated that the fluid was different from the saline solution. This finding eliminated the concern that the seals around the access holes were leaking. It was concluded that the fluid was coming to the surface from the interior of the beams, and was moisture in the concrete that was not removed during the evacuation process prior to encapsulation.

5.1.2 Acoustic Emission Testing

Acoustic emission techniques were used to see if corrosion inside the beams could be detected. The results of theoreticals confirmed other findings and are discussed in Appendix B.

5.1.3 Chloride Content

Results from the chloride content analysis of the beams after completion of exposure testing are compared with the results from the previous study in Table 5.1. The chloride samples for this study were taken from the previously exposed area shown as the "Wet Zone," just outside the area shown as "Dry Zone," and at the end of the beams shown as "End" in Table 5.1. These readings were compared with the readings from the "Wet Zone" in the previous study. It is seen that the levels are similar in the "Wet Zone." Differences are likely due to variability of data within a beam and sampling errors. Some chlorides may have been depleted due to corrosion continuing inside the encapsulated beams. Chloride contents above the threshold for corrosion (0.02-0.05 percent) were found at the ends of five of the six beams. As will be discussed later, corrosion was observed at the ends of the beams.

Table 5.1 Summary of Chloride Content Testing.

		Chloride Content (%)			
		Previous Study	This Study		
Beam	Depth (mm)	Avg. Wet Zone	Avg. Wet Zone	Avg. Dry Zone (Near Wet Area)	Avg. at End
B3	50-75	0.46	0.50	0.55	0.04
	127-152	0.67	0.61	0.74	0.07
B6	50-75	0.77	0.51	0.47	0.03
	127-152	0.88	0.52	0.40	0.07
B12	50-75	0.51	0.56	0.45	0.08
	127-152	0.61	0.56	0.64	0.04
B19	50-75	0.72	0.49	0.06	0.00
	127-152	0.65	0.41	0.14	0.00
B30	50-75	0.74	0.55	0.30	0.03
	127-152	1.06	0.57	0.48	0.05
B34	50-75	1.07	0.44	0.53	0.10
	127-152	0.88	0.85	0.33	0.05

5.1.4 Core Samples and Autopsies

Before the beams were opened for making autopsies, core samples were taken to assess the depth of resin impregnation. From the core samples, it was found that there was no penetration of the epoxy vinyl ester resin except at crack locations where some cracks were partially filled. Some cracks were found without any resin penetration. It was also found that voids near large cracks were not impregnated.

To assess the degree of resin impregnation, six 8 x 12 x 12 in. plain concrete blocks were cast. Two of the blocks were saturated, two were air dried, and two were oven dried before encapsulating and injecting the blocks. After injection, core samples were taken from the specimens to determine the degree of resin penetration into the concrete. It was found that regardless of the curing conditions, there was virtually no resin impregnation unless there was surface cracking due to shrinkage and temperature effects. In most cases, the resin only formed a surface layer and did not penetrate the concrete.

Inspection of the core samples under ultraviolet light made it possible to assess the depth of penetration of the resin. The resin was invisible to the naked eye but glowed in ultraviolet light.

When the beams were opened, a dark green fluid, generally indicative of active corrosion was found along the black (uncoated) bars in all beams. The amount and viscosity of this fluid changed from beam to beam. Figures 5.7 and 5.8 show this corrosion fluid in beams 30 and 34.

Figure 5.7 Green Corrosion Fluid on Beam 30.

Figure 5.8 Green Corrosion Fluid on Beam 34.

A difference in concrete color between previously exposed areas and elsewhere in the beam was consistently found in encapsulated specimens (darker area to the right in Figure 5.9). The "wet" appearance indicated that moisture remained inside the beams and, as a consequence, half-cell potential readings remained stable. Corrosion activity continued inside the encapsulated beams.

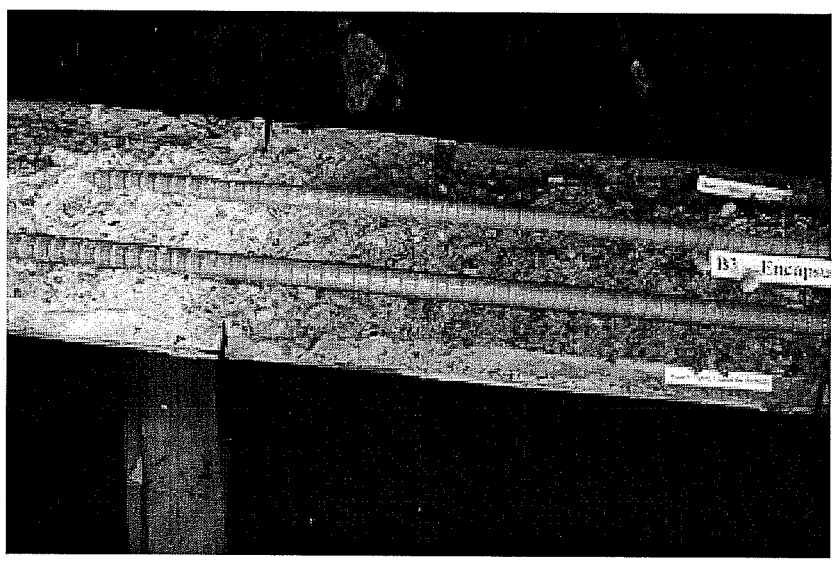

Figure 5.9 Difference in Appearance of Concrete in Beam 3.

Another observation was that the epoxy-coated bars usually performed well while the uncoated bars were severely corroded. Beam 34, which had spliced bars, was the only beam with damage to epoxy-coated bars. The ends of the bars where epoxy was patched were corroded. Other than that, visible damage to the epoxy-coated bars was insignificant. There were some stains near the stirrup in all beams. The stains were probably caused by corrosion of tie wires. In some cases the corrosion extended underneath the epoxy coating and was found only after the epoxy coating was peeled away. The bar surface was mottled with rust. The locations where corrosion was observed under the

coating generally corresponded with the locations of splices, intentionally damaged areas on epoxy coating, intentionally damaged and patched areas on epoxy coating, and crack locations. Figure 5.10 shows how well the epoxy-coated bars performed. Figures 5.11 and 5.12 show the rust stains on and underneath the epoxy coating. Figure 5.13 shows the damage underneath the epoxy coating for Beam 12, while the same bar is seen without any damage in spite of the intentional damage shown in Figure 5.14. These differences were primarily related to crack locations.

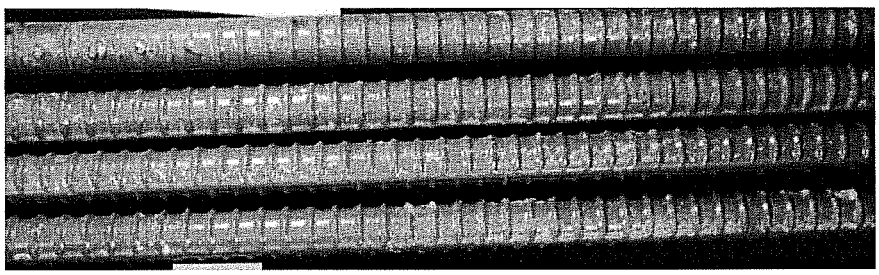

Figure 5.10 Epoxy-coated Bars (Beam 34).

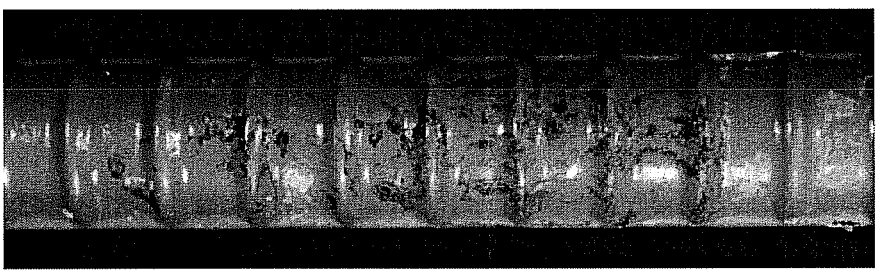

Figure 5.11 Rust Stains on Epoxy-coated Bar (Beam 6).

Figure 5.12 Rust Stains Underneath Coating on Epoxy-coated Bar (Beam 6).

Figure 5.13 Rust Stains Underneath Coating on Epoxy-coated Bar (Beam 12).

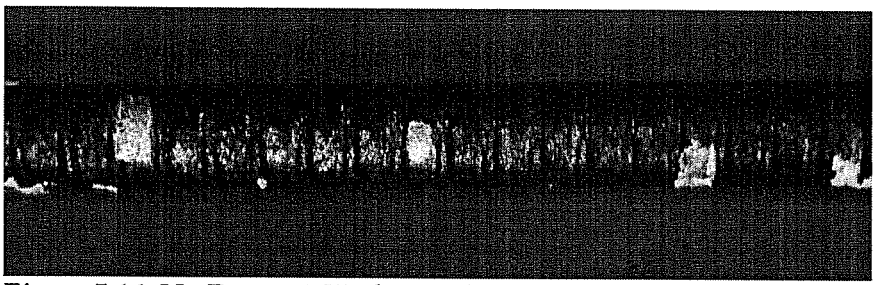

Figure 5.14 No Damage Underneath Coating on Epoxy-coated Bar (Beam 12).

In the uncoated bars of all beams, significant loss of steel areas as well as pitting in several locations was observed. Significant loss of steel area is shown in Figure 5.15 for the Beam 19 bottom black bar near the stirrup, in Figure 5.16 for Beam 6 bottom black bar in the previously exposed region, and in Figure 5.17 for Beam 12 top black bar in the previously exposed area. The loss of bar area shown was typical of the black bars of all the beams. Significant loss of bar area is defined as loss of more than 15-20 percent of the bar area. For the control specimens, corrosion damage extended outside the previously exposed region in the form of pitting (Figures 5.18, 5.19). In pitting corrosion, the profile of the bar remains the same. There are pits that do not significantly (less than 10 percent) change the bar area. For the encapsulated specimens the damage was usually within the previously exposed region. All of the encapsulated specimens, however, showed pitting corrosion at the end of the beams (Figures 5.20, 5.21). It is likely that the ends of the encapsulated beams were not sealed properly around the protruding bars, and corrosion was initiated in regions where no corrosion had occurred earlier. Corrosion activity on the black bars in the encapsulated specimens appeared to be greater than the damage in the control (unencapsulated) specimens.

Figure 5.15 Significant Loss of Bar Area (Beam 19).

Figure 5.16 Significant Loss of Bar Area (Beam 6).

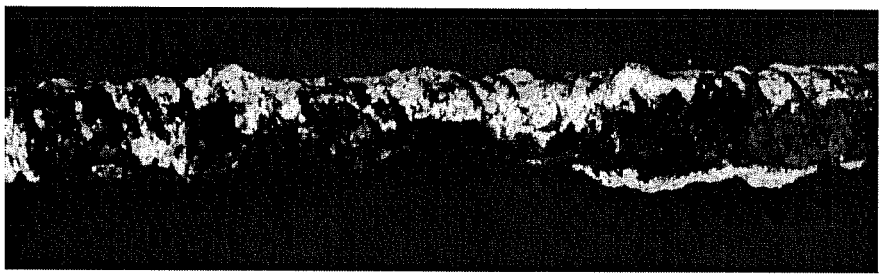

Figure 5.17 Loss of Bar Area (Beam 12).

Figure 5.18 Corrosion Outside the Previous Exposed Region (Beam 12).

Figure 5.19 Corrosion Outside the Previous Exposed Region (Beam 30).

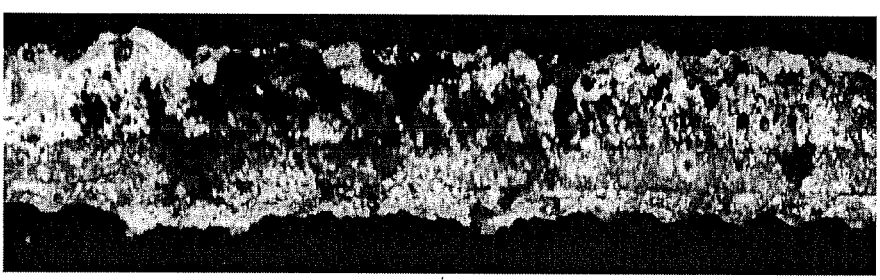

Figure 5.20 Pitting Corrosion at the End of the Bar (Beam 6).

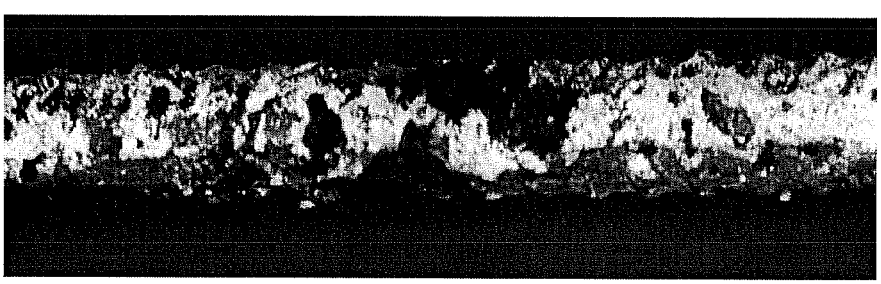

Figure 5.21 Pitting Corrosion at the End of the Bar (Beam 19).

In the three beams where the stirrups were monitored (B19, B30, and B34), significant corrosion damage was observed in the stirrups. There were stains on the epoxy coating, and when the coating was peeled away, rust was found over nearly the total bar surface area. In the previous study it was found that bars bent after coating did not perform well [Vaca, 1998]. Figures 5.22 and 5.23 show the stirrups after removal from the beams. Table 5.2 is a summary of corrosion damage on all six beams.

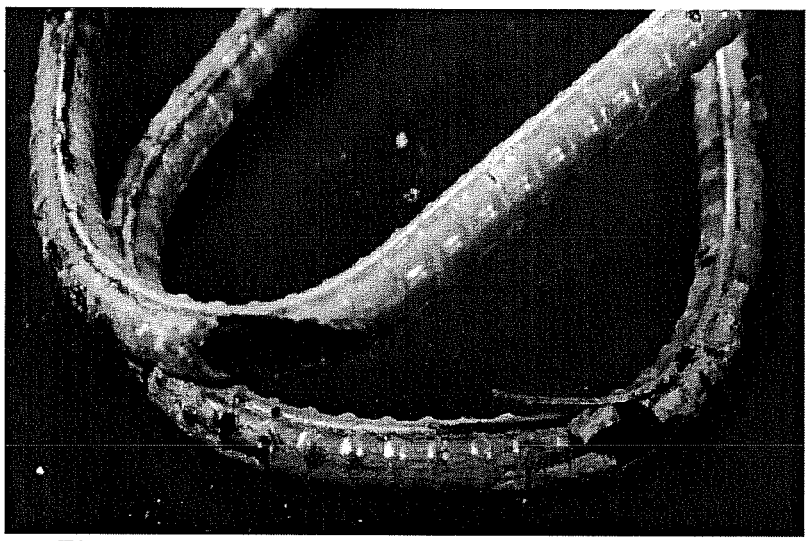

Figure 5.22 Corrosion Damage on Stirrup (Beam 30).

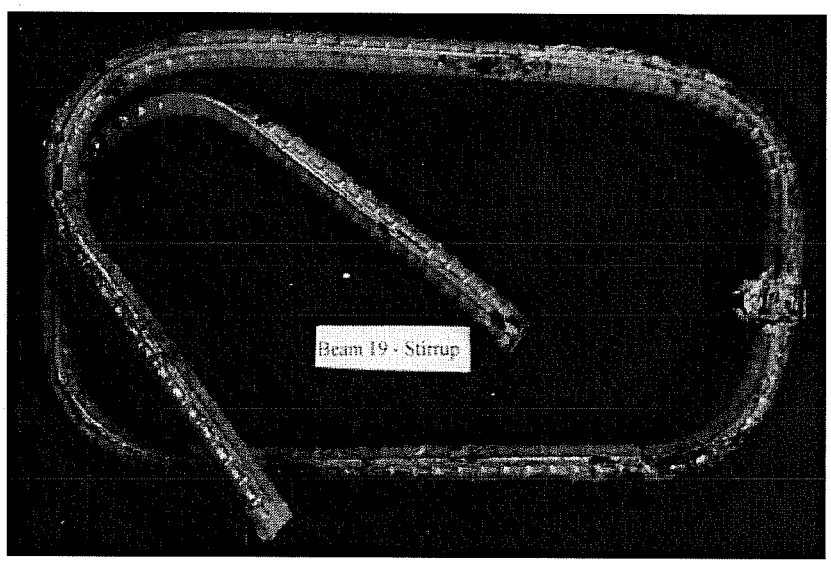

Figure 5.23 Corrosion Damage on Stirrup (Beam 19).

Table 5.2 Summary of Damage Condition of Bars.

		Corrosion Damage		
Beam	**Type**	**Black Bars**	**Epoxy-coated Bars**	**Stirrup**
B3	Encapsulated	Significant loss of bar near stirrup and several other locations in PEA. Pitting at the end.	Bars in good shape. Only stains around the stirrup. Rust was found underneath these stains when epoxy coating was peeled. Insignificant damage.	Not applicable.
B6	Encapsulated	Significant loss of bar area and pitting in PEA. Pitting at the end as well.	Stains in the middle and in the PEA. When epoxy peeled some minor damage was found.	Not applicable.
B12	Control	Significant loss of bar area in PEA. Some pitting and mottled surface outside the PEA and at the end.	Stains at PEA, especially at intentionally damaged locations. Not all locations exhibited corrosion. Some pitting corrosion at PEA.	Not applicable.
B19	Encapsulated	Significant loss of bar area around the stirrup. Pitting at the end.	Not applicable.	Corrosion all around. Pits in the epoxy coating. Damage found especially at the bents when epoxy was peeled
B30	Control	Significant loss of bar area and pitting in several locations extending uniformly through the of bar.	Stains around the stirrup and at locations of patching. Rust was found underneath epoxy coating on these locations.	Coating peeled off in several locations. Bar underneath corroded. Stirrup extensively corroded.
B34	Encapsulated	Significant loss of bar area near the stirrup. Damage extending throughout the PEA with pitting and loss of bar area in several places. Pitting at the end extending towards the PEA.	Long splice bars performed well-some having stains at the splice location. Short splice bars exhibited the most corrosion of all beams. Many stains on epoxy coating and corrosion spread underneath the coating.	Stirrup in the middle was corroded. Pits were found underneath the epoxy coating. Of the two other stirrups at splice locations, one performed well while the other one had some damage, mostly around the corners.

PEA : Previously Exposed Area

5.2 MACRO-CELLS

5.2.1 Half-Cell Potential Readings for Unencapsulated Macro-Cells

Figure 5.24 shows the half-cell potential readings for the unencapsulated macro-cells. These readings were only taken for the control specimens since surface access was not possible for the encapsulated specimens. The readings indicate that the corrosion activity inside these macro-cells increased during the exposure cycles. This was confirmed later by visual observations.

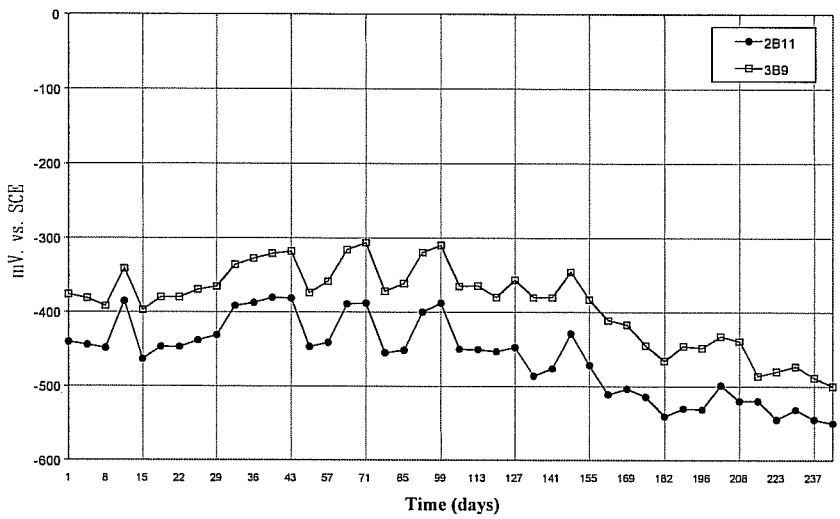

Figure 5.24 Half-Cell Potential reading for Unencapsulated Macro-Cells.

5.2.2 Macro-Cell Potential Readings

The macro-cell potentials throughout the duration of the encapsulation study as well as the previous study is shown in Figure 5.25 through 5.29. The previous study is shown as the TxDOT Program and the encapsulation study is shown as Encap. Program. There was a gap of 9 months between the two studies. Analyzing the data, it is apparent that the polarity of the macro-cells changed during the study. Therefore, the readings are not very useful. The visual observations after opening the macro-cells confirm active corrosion in the black bars and indicate that the cathode and the anode were reversed. Since the macro-cells were designed to work in one direction (with the coated bars serving as the cathode), the change in polarity makes the readings meaningless. It was also noticed in the previous study that the readings became meaningless when the black bars started to corrode [Vaca, 1998].

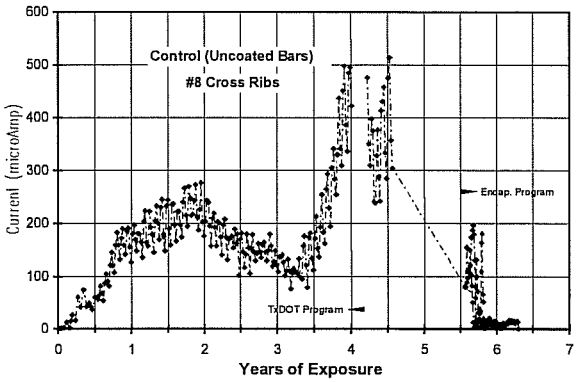

Figure 5.25 Macro-Cell Corrosion Current Readings for Specimen 1B8.

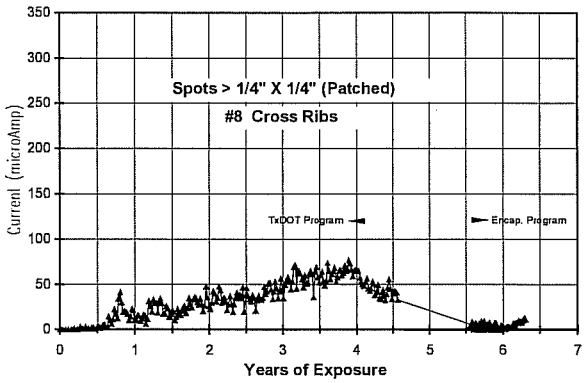

Figure 5.26 Macro-Cell Corrosion Current Readings for Specimen 3B9.

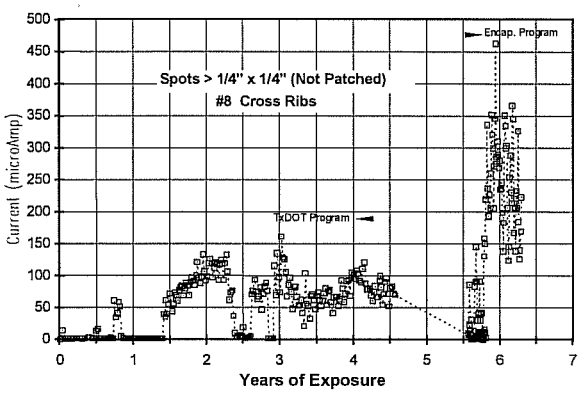

Figure 5.27 Macro-Cell Corrosion Current Readings for Specimen 2B10.

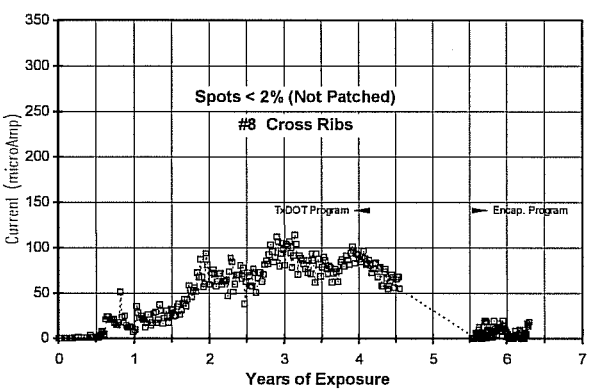

Figure 5.28 Macro-Cell Corrosion Current Readings for Specimen 2B11.

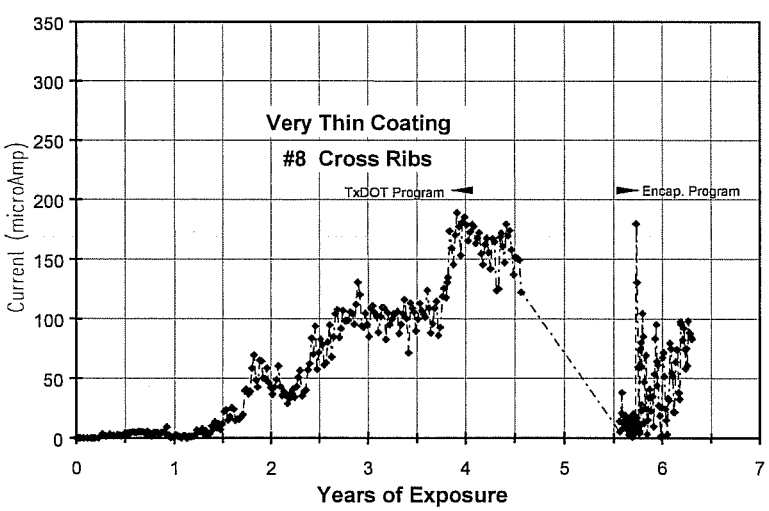

Figure 5.29 Macro-Cell Corrosion Current Readings for Specimen 1B.*

5.2.3 Chloride Content

Results from the chloride content analysis at the end of this study are compared with the results from the previous study in Table 5.3. It is seen that the chloride contents are somewhat lower than those from the previous study.

Table 5.3 Summary of Chloride Content Testing for Macro-Cells.

		Avg. Chloride Content (%)	
Macro-Cell	**Avg. Depth (mm.)**	**Previous Study**	**This Study**
1B8	25-50	0.30	0.18
	75-100	0.20	0.11
1B*	25-50	0.36	0.21
	75-100	0.26	0.14
3B9	25-50	0.34	0.25
	75-100	0.20	0.12
2B10	25-50	0.34	0.14
	75-100	0.22	0.09
2B11	25-50	0.38	0.29
	75-100	0.30	0.10

5.2.4 Autopsies

When the macro-cells were opened, a green fluid was found in all the macro-cells on and near the straight black bars and on the bent black bar. 5.30, 5.31, and 5.32 show the fluid and stains on specimens 2B11, 3B9, and 2B10. Figure 5.33 shows the fluid staining the concrete after removing the bent black bar from specimen 1B8.

Figure 5.30 Corrosion Stains and Active Corrosion on Black Bars (2B11).

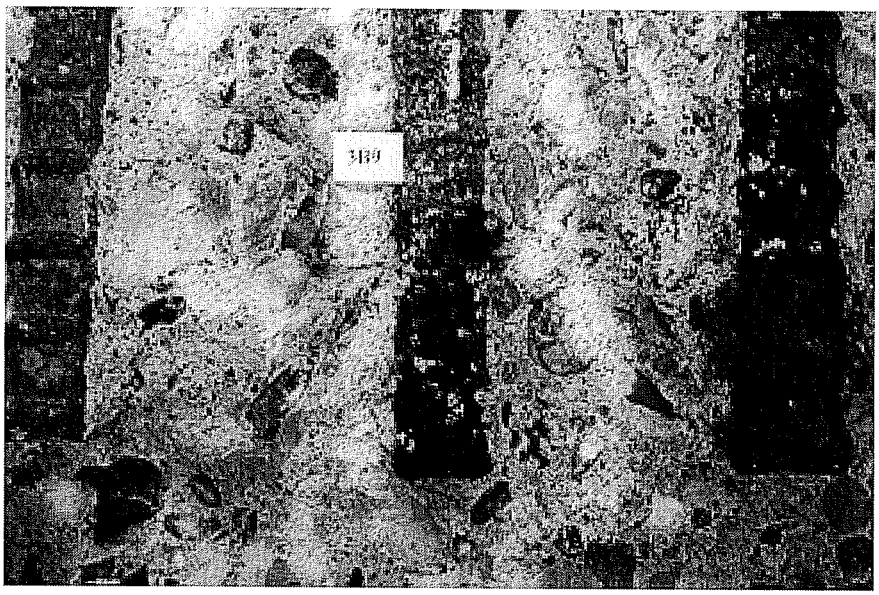

Figure 5.31 Corrosion Stains and Active Corrosion on Black Bars (3B9).

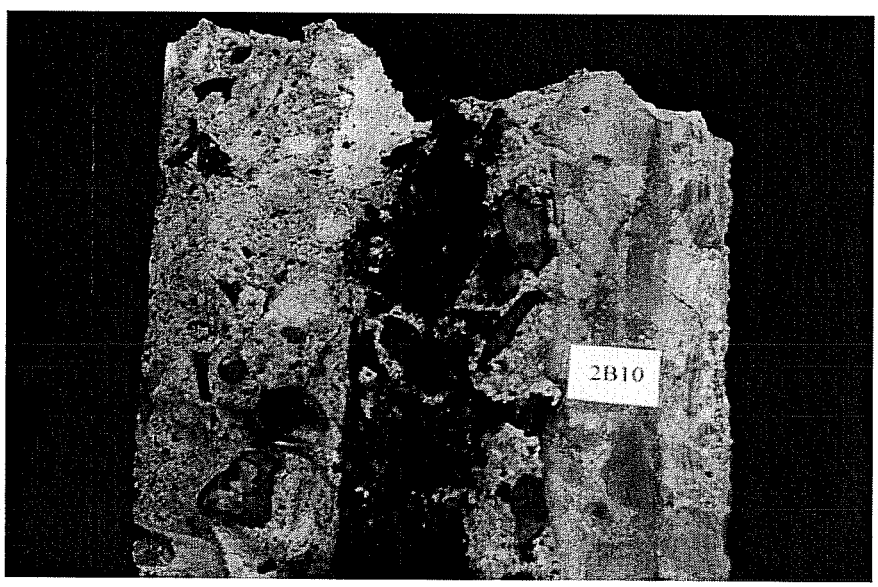

Figure 5.32 Corrosion Stains and Active Corrosion on Concrete (2B10).

Figure 5.33 Active Corrosion on Concrete Bent Black Bar Side (1B8).

Considerable pitting damage was found on black bars and on epoxy-coated bent bars. Figures 5.34 and 5.35 show the pitting corrosion on the black bent bar and the severely stained concrete after this bar was removed. Similarly, Figures 5.36 and 5.37 show the pitting corrosion on epoxy-coated bent bar and concrete stains after the bar was removed.

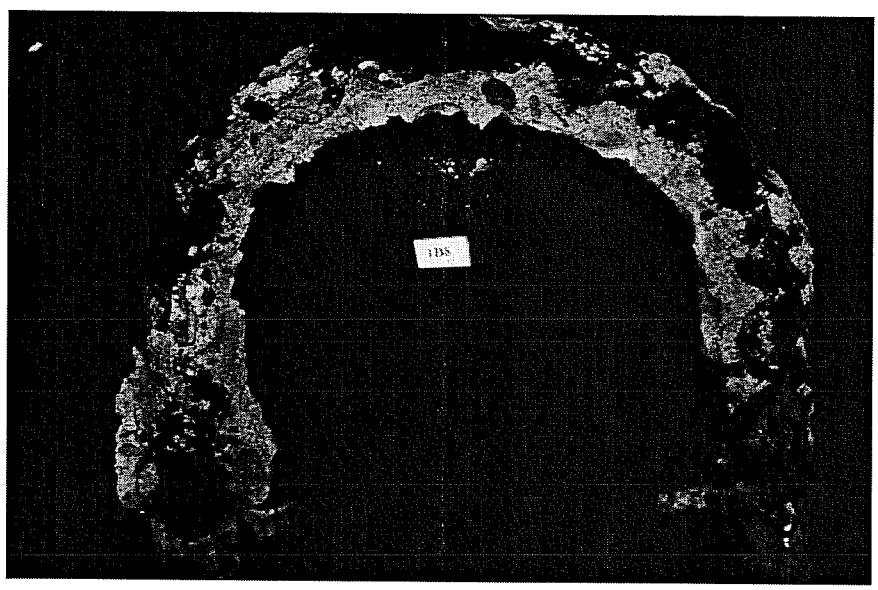

Figure 5.34 Damage on Bent Black Bar (1B8).

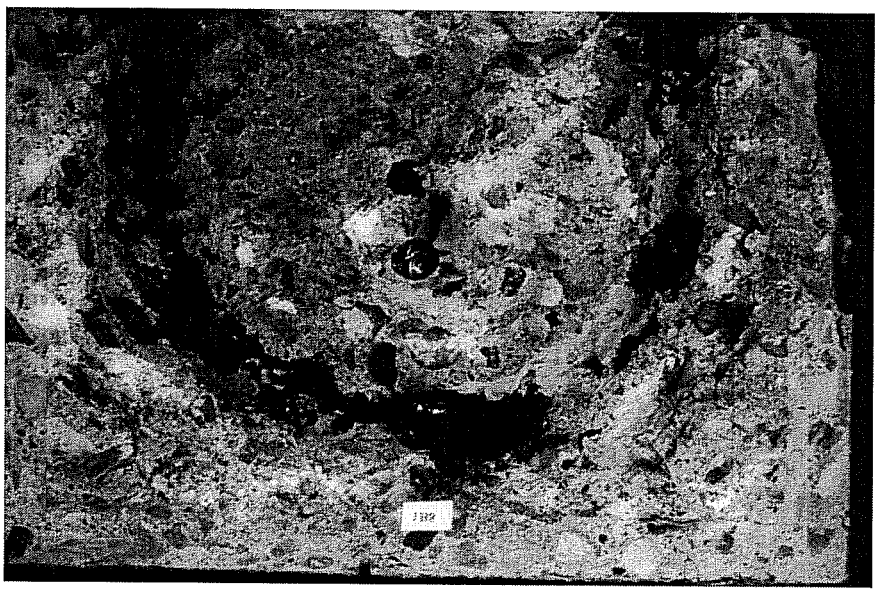

Figure 5.35 Damage on Concrete for Bent Black Bar (1B8).

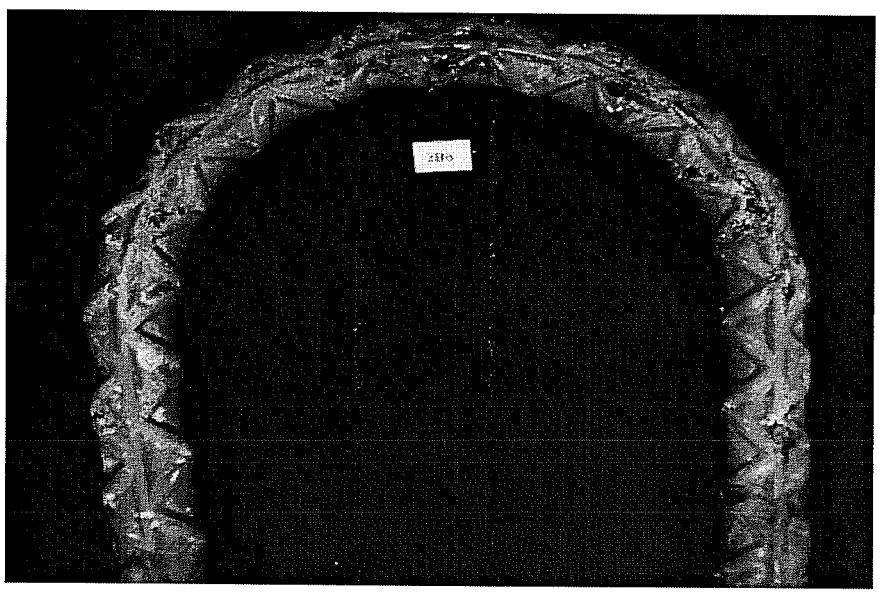

Figure 5.36 Pitting Damage on Epoxy-coated Bent Bar (3B9).

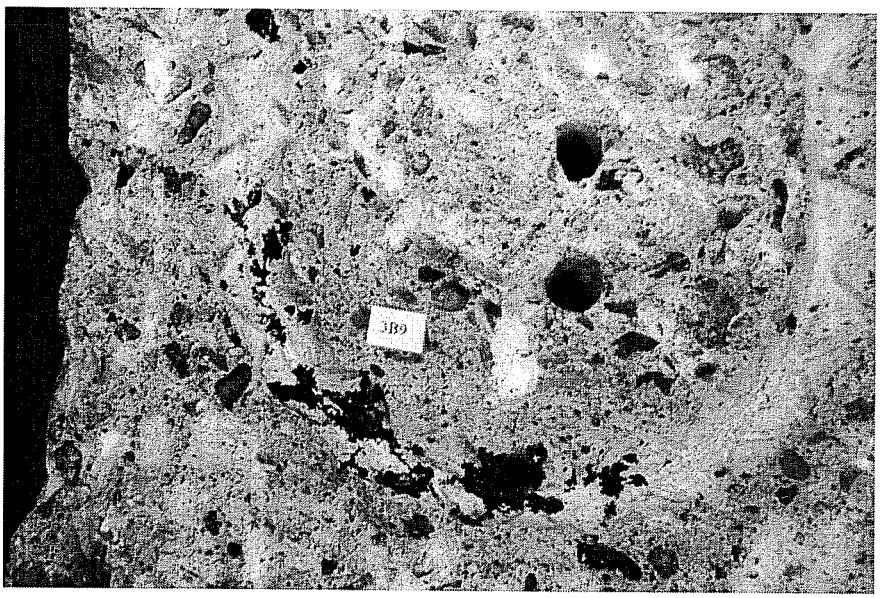

Figure 5.37 Damage on Concrete for Epoxy-coated Bar (3B9).

Figure 5.38 shows corrosion stains on the concrete surface after the distribution medium were peeled away. Corrosion may advance beneath the encapsulated surface but is not visible since the distribution medium masks the stains. In field applications, encapsulation may eliminate the possibility of inspecting the surface for signs of corrosion.

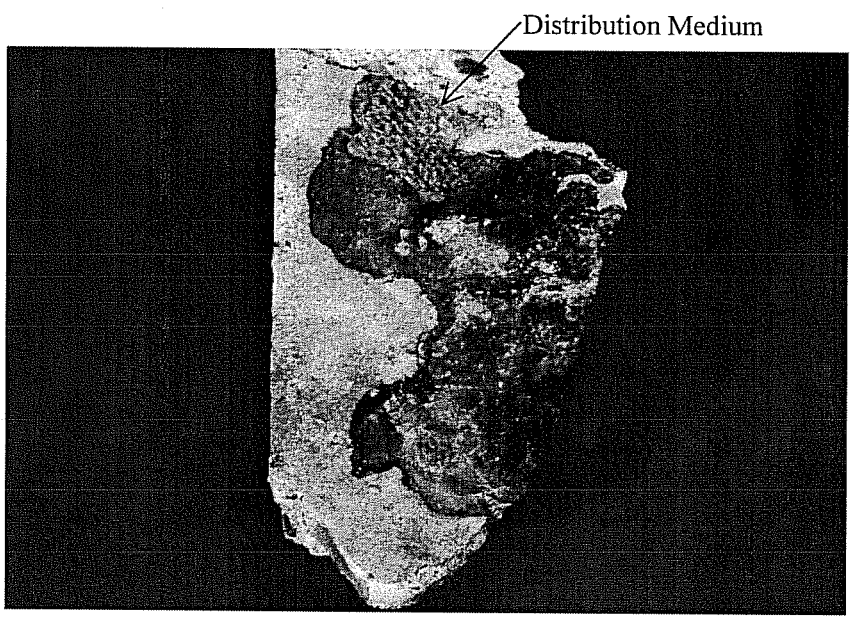

Figure 5.38 Corrosion Stains Underneath Epoxy and Distribution Media.

CHAPTER 6

SUMMARY AND CONCLUSIONS

6.1 SUMMARY

The importance of repair and rehabilitation of corrosion damaged structures is increasing because the deterioration rate of existing structures increases as they age. New ways to protect against corrosion and new methods to repair corrosion damage in the most efficient way need to be developed and studied.

A rehabilitation technique involving encapsulation and epoxy vinyl ester resin injection was studied. The technique was used on specimens that had been exposed to a corrosive environment for four and a half years. Well-documented, advanced corrosion was evident in the beams. The behavior of specimens encapsulated and injected with resin was compared with specimens with no repair. All specimens were exposed to a corrosive environment for one year. The specimens were monitored by taking half-cell potential readings during the exposure period. At the end of the study, all specimens were examined (bars removed) to assess the condition of the reinforcement.

6.2 OVERVIEW OF THE TEST RESULTS

From the six beams tested (4 encapsulated, 2 control), the following observations were made:

- Half-cell potential readings taken at intervals throughout the exposure period indicated corrosion activity in all beams.
- Autopsies conducted at the end of the exposure period showed active areas of corrosion (green corrosion fluid) for both encapsulated and control specimens around the black bars. Also, the concrete in the previously exposed area had a darker, more glistening appearance in the encapsulated specimens than the same area in the control specimens.
- Epoxy-coated reinforcement performed well on both encapsulated and control specimens.
- Black (uncoated) bars performed poorly with loss of cross section area especially in the previously exposed region. There appeared to be more damage in the encapsulated specimens compared to the control specimens.
- Black bars in the encapsulated specimens showed pitting corrosion near the ends of the beams, a location where it had not occurred during the previous four and a half year exposure study nor on the control specimens in this study.
- Black bars in the control specimens exhibited corrosion over nearly their entire length, but the most severe damage was found in the previously exposed area.
- Significant corrosion damage was observed in the stirrups. Rust stains were found on the epoxy coating and damage extended underneath the coating.
- Cores taken from the encapsulated specimens to determine depth of penetration of epoxy vinyl ester resin indicated that there was no significant penetration.

From the five macro-cells tested (3 encapsulated, 2 control) the following observations were made:

- There was no difference between the encapsulated and control specimens in terms of damage. All macro-cells showed signs of active corrosion (green corrosion fluid) when autopsies were performed.
- Macro-cell potential readings were inconclusive due to the change in polarity (corrosion of bottom rather than top bars in the macro-cell). However, half-cell potential readings indicated corrosion was continuing in the control specimens.

6.3 Conclusions

Based on the experimental results from this project, the following conclusions were made:

- The use of a fiber reinforced composite shell coupled with epoxy vinyl ester resin injection was not effective in arresting active corrosion in beams damaged from exposure to a corrosive environment for four and a half years prior to repair. The performance of concrete elements similarly encapsulated prior to any exposure and with no corrosion damage could not be assessed in this study.
- Evacuation of the concrete specimens did not remove moisture from the beams and vacuum injection of resin did not result in penetration of resin other than at large cracks. It is likely that most of the moisture was trapped inside during encapsulation. Since there was already sufficient oxygen and chlorides in the concrete, corrosion continued at about the same rate as before repair.
- The encapsulation process covers the concrete surface and eliminates the possibility of inspecting a structural element for rust stains or other signs of corrosion.
- Epoxy-coated bars performed well in all specimens. Uncoated bars showed considerable corrosion damage in both control and encapsulated specimens.

6.4 Recommendations For Further Research

Further study is needed to better understand the effectiveness of encapsulation and epoxy injection for corrosion protection or rehabilitation of damaged elements. The removal of moisture from concrete, effectiveness of resin impregnation and mechanism of corrosion in an encapsulated element are not well understood.

Further research on use of acoustic emission methods for monitoring onset of corrosion is encouraged. The limited data from this study was promising.

APPENDIX A

*PROPERTIES OF HARDSHELL-CSRS PROCESS MATERIALS**

Description: Product Data Sheet for the Hardshell Concrete Restoration System
Rev: A
Date: 12/5/96

1.0 System Description

1.1 Prefabricated E-glass shells are adhesively bonded to concrete structures to contain spalling, provide additional strength, extend life expectancy, and upgrade aesthetics. Thickness and orientation of shells is dependent on application. Entire system is coated with a methyl methacrylate coating.

2.0 Component Properties

2.1.0 The system components include: E-glass fabric, matrix resin, adhesive resin, and methyl methacrylate coating

2.1.1 E-glass fiber reinforcements

Typical aerial weights

0 Deg. Continuous Strand Roving	24.00 oz/yd^2	5.0% deviation
90 Deg. Continuous Strand Roving	16.00 oz/yd^2	5.0% deviation
+45 Deg. Continuous Strand Roving	12.00 oz/yd^2	5.0% deviation
- 45 Deg. Continuous Strand Roving	12.00 oz/yd^2	5.0% deviation
Mat	06.75 oz/yd^2	5.0% deviation
Stitch Yarns	00.05 oz/yd^2	5.0% deviation

2.1.2 Composite matrix resin (Derakane 411-350)

Typical clear cast properties

Tensile Strength	11000 psi.
Tensile Modulus	0.49 msi.
Compressive Strength	16000 psi.
Compressive Modulus	3.5 msi.
Elongation	5 %
Barcol Hardness	35

2.1.3 Adhesive Resin (Derakane 8084)

Typical mechanical properties

Property	**Test Method**	**Test Value (Tested at 77 deg. F)***
Lap Shear Strength (Fiberglass Composite Substrate)	ASTM D 1002	900 psi
Tensile Strength	ASTM D 638	10-11,000 psi.
Elongation	ASTM D 638	10-12 %
Heat Distortion temp	ASTM D 4065	170-180 deg. F
Barcol Hardness	ASTM D 2240	30

* Reproduced from suppliers Product Data Sheet.

2.1.4 Methyl methacrylate coating (Eliminator S)

Typical mechanical properties

Property	Test Methods	Units
Water Vapor Transmission	ASTM 96-80	6.6 g/m^2/day
Adhesion to concrete	ASTM D4541	100psi
Adhesion to Steel	ASTM D4541	290 psi
Minimum Tensile Strength	ASTM D638	940 psi
Elongation	ASTM D638	80%

3.0 Laminate Information

3.1 All composite plates and angles are fabricated in a factory environment using the SCRIMP process (Seemann Composites Resin Infusion Molding Process). The SCRIMP process is a closed process that is highly reproducible. The vacuum driven process results in composites with low void and high fiber volume.

3.2 Fiberglass composite mechanical properties

Property at 72 deg. F	Test Method	Test Value
Tensile Modulus	ASTM D 3039	3.75 Msi.
Ultimate Tensile Strength	ASTM D 3039	70 ksi.
Strain	ASTM D 638	2.0 %
Fiber Volume Fraction	ASTM D 3171	54 %
Tg Composite Shells	ASTM D 4065	150 deg. F

4.0 Fiberglass adhesion information

4.1 All bonding surfaces are to be sandblasted for improved adhesion with the Derakane 8084. The sandblast must be uniform on the composite surface. The composite must be sandblasted with a fine grit sand until the fiberglass composite is feathered white.

4.2 Bond lines shall range from .03125" through .1875".

4.3 Minimum joint lap length for plate / angle lap joints is 4".

5.2 No infusion shall be performed below 40 deg. F or above 100 deg. F.

5.8 All infusion ports shall be filled and coated with an epoxy or methyl methacrylate coating.

APPENDIX B

CORROSION DETECTION IN REINFORCED CONCRETE BEAMS USING ACOUSTIC EMISSION

B.1 CORROSION DETECTION IN REINFORCED CONCRETE USING ACOUSTIC EMISSION

Corrosion produces stress waves that can be picked up by acoustic emission sensors. These stress waves may be generated by corrosion processes such as surface film growth and fracture, concrete matrix cracking, and cathodic bubble noise or by damage to the materials which might become emissive when subjected to stress from sources such as area reduction, cracking, and pitting [Fowler, 1997; Pollock, 1986; Landis, 1994]. Also Weng *et al.* [1982], report that acoustic emission from corroding and non-corroding specimens are different and that acoustic emission from corroding specimens is probably due to hydrogen gas evolution.

Research conducted at Northwestern University by Zdunek *et al.* show that early detection of steel rebar corrosion by acoustic emission is possible by using the steel as a waveguide. Researchers have also indicated that acoustic emission can detect corrosion earlier than other traditional electric current measurements [Pollock, 1986; Landis, 1994; Zdunek, 1995].

B.2 ACOUSTIC EMISSION APPLICATION TO THE BEAMS

Acoustic emission testing of the beams was performed according to the Standard Procedure of Acoustic Emission Evaluation used by the Association of American Railroads. The testing was performed using 60 kHz and 150 kHz sensors which were attached to bars protruding from the concrete. The steel was used as a waveguide to eliminate attenuation problems encountered when sensors are attached to concrete.

Before the sensors were attached, the surface of steel bars was smoothed at the sensor location. The sensors were attached using high temperature hot melt glue. The standard procedure for acoustic emission evaluation involves breaking a pencil lead six inches away from the face of the sensors in order to verify their function and to characterize attenuation. Pencil lead fracture at other bars in the same beam was picked up by the sensor which indicates that corrosion on any bar can be detected by a single sensor on the element, at least for this particular beam reinforcement configuration. However, a different result might be found for field applications, especially in large specimens, due to different attenuation characteristics.

After the system was calibrated, corrosion was monitored continuously for three days. The system was also monitored during the periodic loading and unloading of the beams.

Figures B.1 and B.2 show the typical wave form for a hit obtained during the test. Figure B.3 shows the correlation plot after filtering the data obtained from the acoustic emission testing. The data obtained at the end of the acoustic emission testing program indicated that corrosion was occurring. The hits were short duration, medium amplitude (40-60 dB) and occurred in bursts of emission as expected from results of other corrosion tests in which acoustic emission was used.

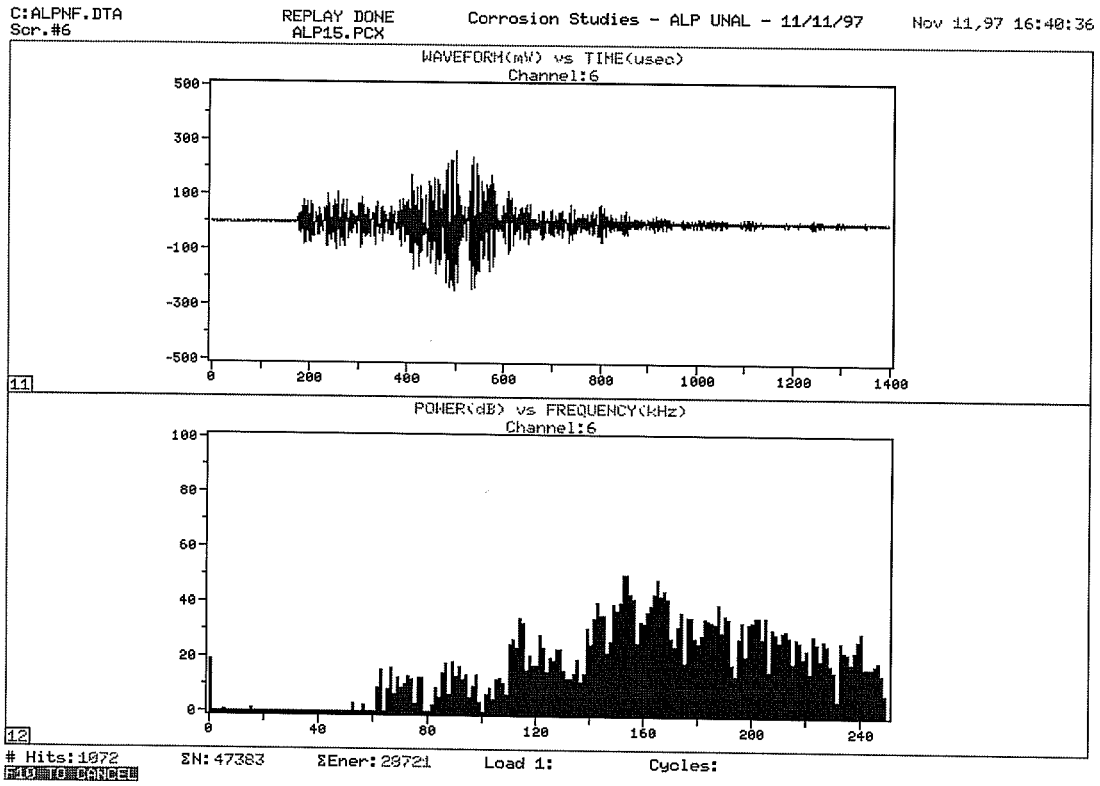

Figure B.1 Typical Wave Form.

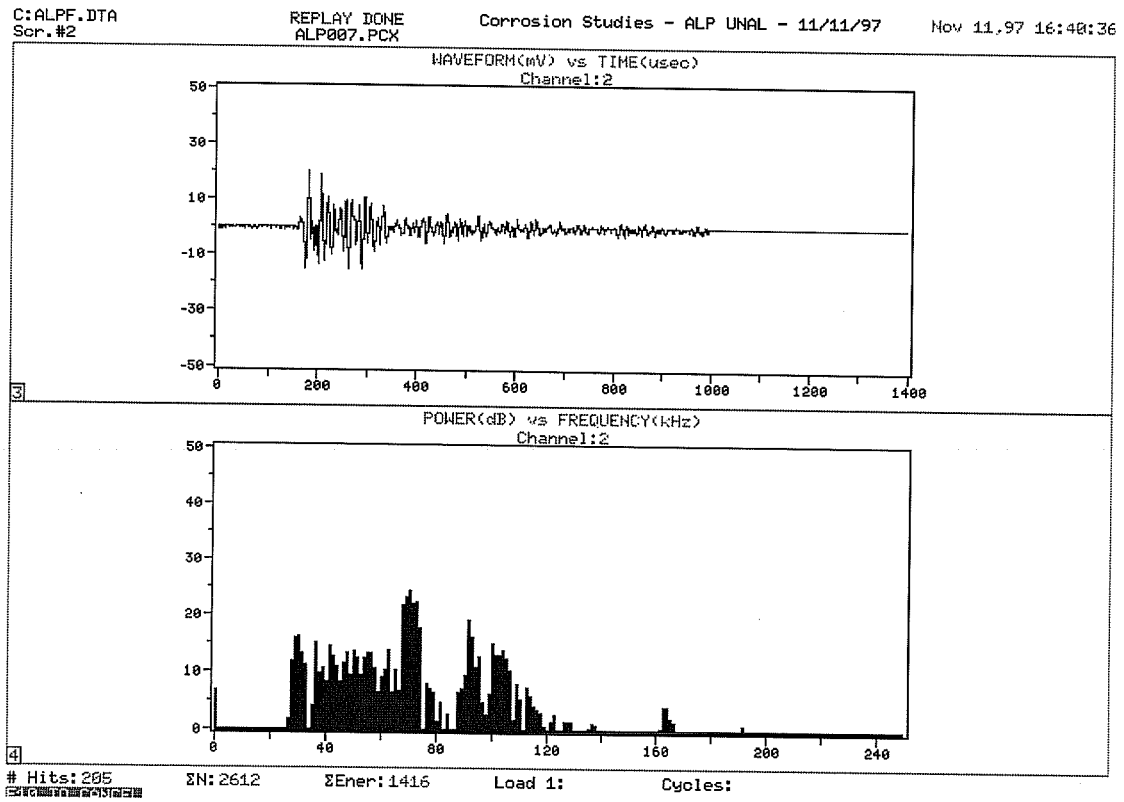

Figure B.2 Typical Wave Form.

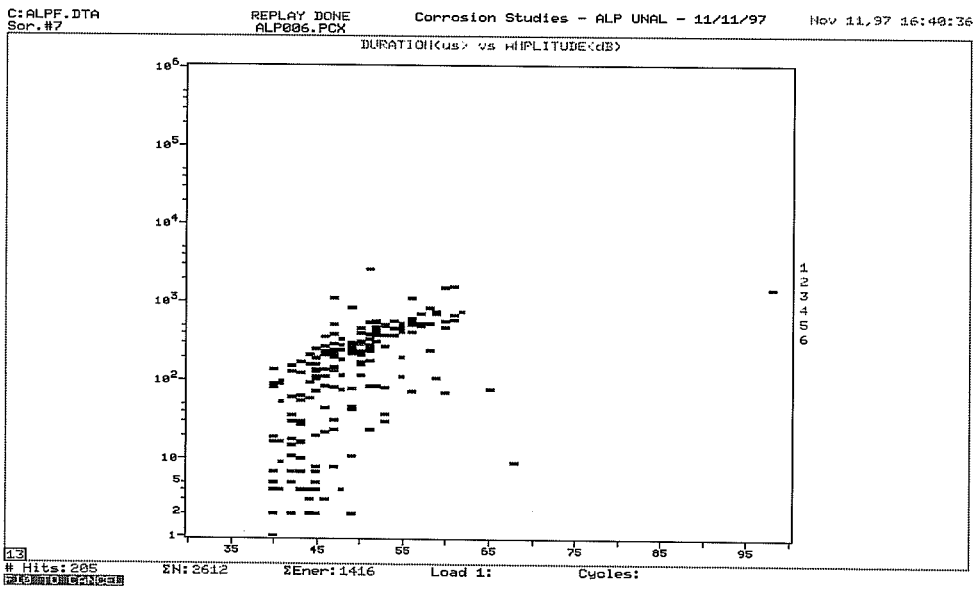

Figure B.3 Correlation Plot.

Figures B.4 and B.5 show typical hits during loading of the beams. Figure B.6 is a correlation plot obtained during loading and loading of the beams. The hits were short duration and medium amplitude and the wave forms indicated occurrence of corrosion. The data shows accelerated corrosion occurring during loading and unloading. The wave forms were not produced by cracking or damage to concrete due to loading since such damage generates emission of high amplitude (70-80 dB) and short duration. After the loading and unloading process, the beams were quiet (no emission) for some time.

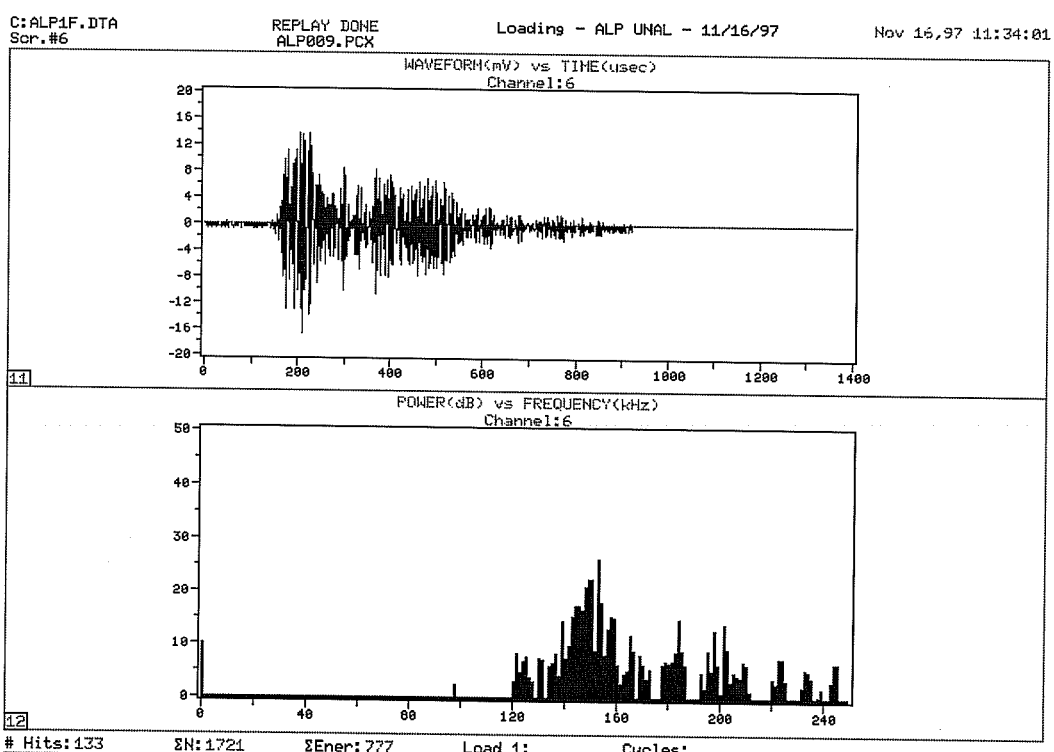

Figure B.4 Typical Wave Form During Loading.

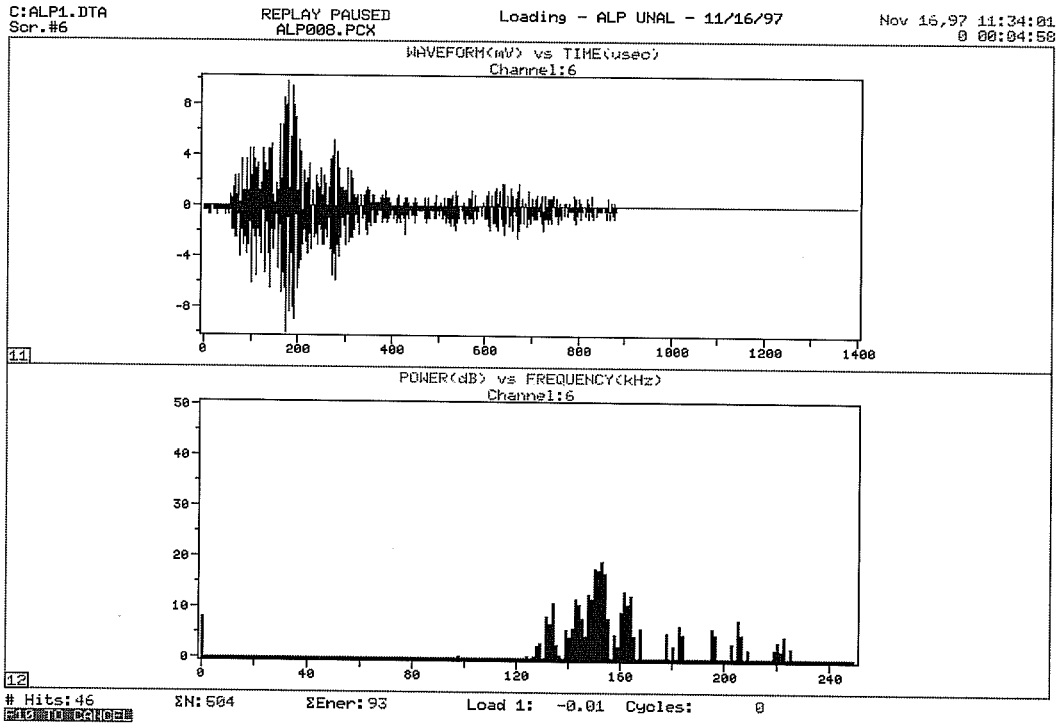

Figure B.5 Typical Wave Form During Loading.

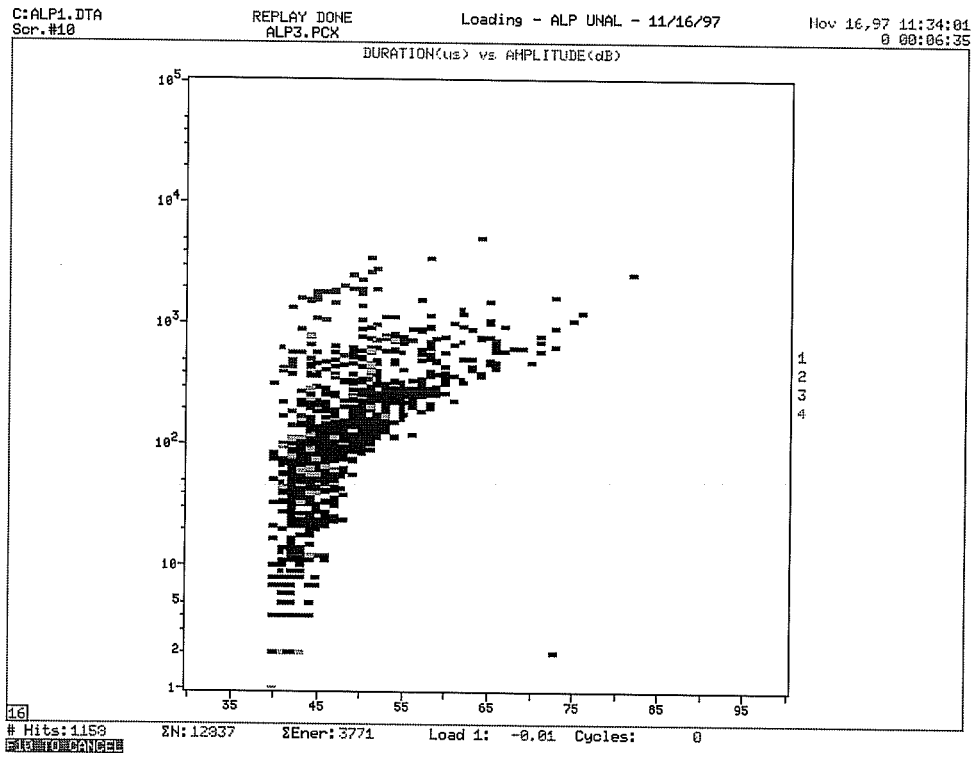

Figure B.6 Correlation Plot During Loading and Unloading.

The data obtained from the acoustic emission testing of beams show similarities with the research conducted at Northwestern University by Zdunek *et al.* which also utilized steel bars as a waveguide [Landis, 1994; Zdunek, 1995]. When the wave forms in Figure B.1 are compared with the wave forms from the research conducted at the Northwestern University (Figure B.7), the similarity is obvious.

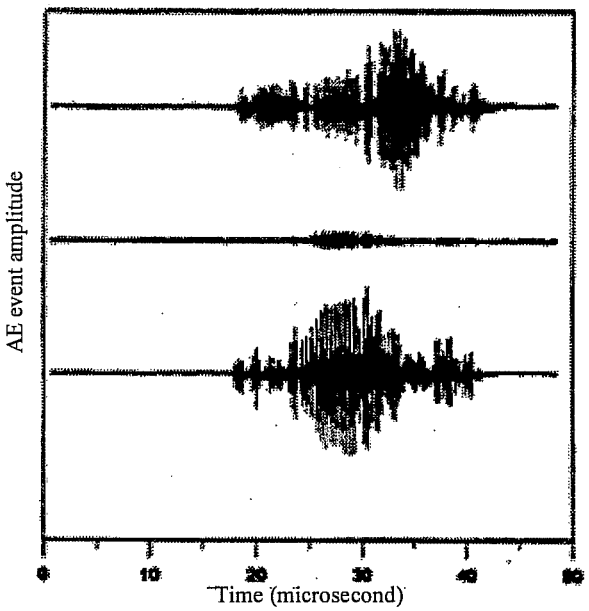

Figure B.7. AE Signal At Three Sensors for a Single AE Hit [Zdunek, 1995].

REFERENCES

Corrosion: Causes and Prevention, Speller, F. N., McGraw-Hill, New York, 1952.

Corrosion Engineering, Fontana, M. G., McGraw-Hill, New York, 1986.

Gibson, F. W. (Editor), "Steel Corrosion in Concrete: Causes and Restraints," ACI Publication SP-102, 1987.

Nene, R. L., "Repairs and Restoration of Reinforced Concrete Columns," ACI Publication SP-85-12, 1985, pp 260–263.

Gallegos, H., Quesada, G., "A Corrosion Case: Repair Procedure," Concrete International, June 1987, pp 54–57.

Pfeifer, D. W., "Steel Corrosion Damage on Vertical Concrete Surfaces–Part I. Causes of Corrosion and Useful Evaluation Tests," ACI Publication SCM-8, 1985, pp 117–119.

Pfeifer, D. W., "Steel Corrosion Damage on Vertical Concrete Surfaces–Part II. Causes of Corrosion and Useful Evaluation Tests," ACI Publication SCM-8, 1985, pp 120–124.

Maurisin, S. L., "Repairs of Concrete Columns, Spandrels, and Balconies on a High Rise Housing Complex in Chicago," ACI Publication SCM-8, 1985, pp 178–186.

Roberts, J. E. "Composite Construction in California Bridge Seismic Retrofitting," California Department of Transportation, Draft Special Provisions, 1997.

Fowler, T., "Class Notes," Austin, 1997.

Pollock, A. A., "Acoustic Emission Capabilities and Applications in Monitoring Corrosion," ASTM Publication STP-908, 1986.

Weng, M. S., *et al.*, "Application of Acoustic Emission to Detection of Reinforcing Steel Corrosion in Concrete," National Association of Corrosion Engineers, Vol. 38, No. 1, January, 1982.

Landis, E., *et al.*, "Development of NDE of Concrete," Northwestern University Center for Advanced Cement-Based Materials and BIRL Industrial Research Laboratory, June 1994.

Zdunek, A. D., *et al.*, "Early Detection of Steel Rebar Corrosion by Acoustic Emission Monitoring," National Association of Corrosion Engineers International Annual Conference and Corrosion Show 1995, Paper No. 547.

Kahhaleh, K. Z., "Corrosion Performance of Epoxy-Coated Reinforcement," Ph.D. Dissertation, The University of Texas at Austin, May 1994.

Vaca, E., "Epoxy Coated Bars Corrosion," Ph.D. Dissertation, The University of Texas at Austin, May 1998.

American Society for Testing and Materials, "Half-Cell potentials of Uncaoted Reinforcing Steel in Concrete," ASTM C876-87, Philadelphia, PA, 1987.